

Article

From Polyolithic to Monolithic: The Design of a Lightweight, Stiffened, Non-Rotational, Deep-Drawn Automotive Product

Gibson P. Chirinda ^{1,*} , Stephen Matope ¹, Andreas Sterzing ² and Matthias Nagel ²

¹ Department of Industrial Engineering, Faculty of Engineering, Stellenbosch University, Private Bag X1, Matieland, Stellenbosch 7602, South Africa; smatope@sun.ac.za

² Fraunhofer Institute of Machine Tools and Forming Technology IWU, Reichenhainer Straße 88, 09126 Chemnitz, Germany

* Correspondence: 24588636@sun.ac.za or gibbschirinda@gmail.com; Tel.: +27-66-545-4157

Abstract: The transition from polyolithic (composed of many parts) to monolithic (one part) design in automotive components presents an opportunity for a reduction in part count, weight, processing routes, and production time without compromising performance. The traditional design approaches for rooftop tents assemble various sheet metal and extrusions together using different joining processes such as welding, adhesive bonding, bolting, and riveting. This is often associated with disadvantages, such as increased weight, high production time, and leaking joints. This research, therefore, presents the development of a monolithic, lightweight, stiffened, non-rotational automotive rooftop tent that is manufactured via the deep-drawing process. An onsite company case study was conducted to analyze the polyolithic product and its production process to determine its limitations. This was followed by the design of a lightweight, non-rotational monolithic product whose purpose is to eliminate the identified disadvantages. The stiffness geometries were developed to enhance the overall structural integrity without adding unnecessary weight. The Analytic Hierarchy Process (AHP) was used to analyze and evaluate alternative layouts against criteria such as complexity, tool design, symmetry, rigidity, and cost. Simulations conducted using NX 2024 software confirmed the effectiveness of this design. The results show that the monolithic rooftop tent has a comparable stiffness performance between the lightweight, monolithic rooftop tent and the heavy, polyolithic rooftop tent. At the same time, the part count was reduced from twenty-three (23) single parts (polyolithic) to a one (1) part (monolithic) rooftop tent, the weight was reduced by 15.6 kg, which translates to a 30% weight reduction without compromising the performance, processing routes were reduced from eight (8) to three (3), production time was reduced by 120 min, and leaking was eliminated. It can, therefore, be concluded that the design and manufacturing of monolithic rooftop tents leads to a lighter and stronger product.

Keywords: polyolithic; monolithic; lightweight design; automotive industry; deep drawing



Citation: Chirinda, G.P.; Matope, S.; Sterzing, A.; Nagel, M. From Polyolithic to Monolithic: The Design of a Lightweight, Stiffened, Non-Rotational, Deep-Drawn Automotive Product. *Designs* **2024**, *8*, 123. <https://doi.org/10.3390/designs8060123>

Academic Editor: Yuping He

Received: 15 October 2024

Revised: 12 November 2024

Accepted: 19 November 2024

Published: 21 November 2024



Copyright: © 2024 by the authors. Licensee MDPI, Basel, Switzerland. This article is an open access article distributed under the terms and conditions of the Creative Commons Attribution (CC BY) license (<https://creativecommons.org/licenses/by/4.0/>).

1. Introduction

Reducing vehicle weight without compromising on performance is a key factor in improving fuel efficiency and lowering carbon emissions [1]. This has led to an ever-increasing interest in innovative design and manufacturing techniques that can produce lightweight components without compromising the safety of the passengers, the performance of the vehicle, and the durability of the parts [2]. The transition from polyolithic to monolithic design in automotive sheet metal components presents an opportunity for a reduction in part count, weight, processing routes, and production time without compromising performance [3]. A polyolithic design is one that is made of many parts that are joined together in various manufacturing steps. A monolithic design, on the other hand, is made of one part and eliminates the need for any joining process, thereby streamlining the manufacturing process [4].

1.1. The Current Challenges

While the transition from a polyolithic to a monolithic design is common for small sheet metal products [5], it presents challenges for large products in terms of how to achieve comparable stiffness so that the product does not fail when forces are exerted on it. Once the sheet metal is spread over a large area, it requires stiffeners to support the high-loaded areas. If it does not have the stiffeners, it becomes susceptible to bulging. In some instances, its shape gets distorted, especially on its longer sides. This loss of shape is undesirable and often leads to loss of structural integrity, reduced aesthetic appeal, and increased risk of damage from external forces. As a result, the traditional design approaches for rooftop tents assemble various sheet metal and extrusions together using different joining processes such as welding, adhesive bonding, bolting, and riveting [6]. This, although being a solution to the bulging problem, is often associated with disadvantages, such as increased weight, high production time, and leaking joints. Additionally, the joined points become points of potential failure [7].

1.2. Previous Research

There are previous studies that focused on the effectiveness of monolithic designs in the automotive industry. Hassan and Biswas [8] conducted a study on weight reduction and the monolithic design of a seatbelt bracket that was subsequently manufactured via the additive manufacturing process. The number of parts was reduced from four (4) to one (1), and the one-piece bracket was 77% lighter than the original bracket assembly. In conventional polyolithic assemblies, the multiple sheet metal parts contribute to increased weight. Also, the bolts, nuts, rivets, and other joining materials that are used contribute to the weight of the final product [4]. The monolithic design eliminates these disadvantages and offers a seamless integration into one lightweight part. Other research focused on the application of optimization algorithms to reduce the weight of the body in white (BIW) while at the same time increasing the stiffness. Zhou et al. [9] achieved an 8.5% weight reduction and an increase in stiffness of 11.3% upon the application of an uncertainty optimization technique that considered the deviations in plate thickness, elastic modulus, and welding spot diameter. Takagaki et al. [10] combined structural optimization techniques of topology optimization and shape optimization to reduce the mass of a railway car body by 17% while improving the stiffness by 12%. There is a need to reduce the number of iterations that do not add value to the optimization process. Hao et al. [11] integrated human decision-making with optimization algorithms in a human-in-the-loop optimization method for lightweight vehicle body design (HIL-VBLD). This led to a 12.5% reduction in weight and a reduction in the number of iterations by 23.9%.

The realization of a significant reduction in weight after reducing the number of parts shows the importance of shifting from polyolithic to monolithic designs in an industry that is facing strict environmental regulations to reduce fuel consumption and carbon emissions [12]. Stiffness geometries can be introduced in monolithic designs without significantly increasing material usage, achieving weight reduction while maintaining structural integrity. It is also important to note that other researchers have explored how different design modifications can mitigate damage under extreme loading conditions. Yuen and Nurick [13] presented an experimental and numerical investigation that focused on the deformation and tearing of uniformly blast-loaded built-in quadrangular stiffened plates. The results show that the stiffeners had the effect of reducing the deformation of the plates. Their findings contribute to a broader understanding of energy absorption mechanisms in stiffened structures.

Designing for increased stiffness on shell structures is another important aspect of sheet metal work in the automotive industry [14]. Bambach et al. [15] used the additive manufacturing technique of laser cladding to reinforce and increase the stiffness of a sheet metal component produced via the forming process. Two methods were considered: (1) performing the forming process first, followed by the application of laser cladding at the corners of the product, and (2) conducting the laser cladding on sheet metal before the

forming process commences. The findings show that even though this reduces formability, the application of additive manufacturing in sheet metal products has the potential for stiffness management in formed products and the production of tailored laser-clad blanks.

Scheffler et al. [16] conducted incremental sheet metal forming on the exterior parts of a streamlined vintage concept car. The selected parts are manufactured via deep drawing (roof panel), hydroforming (bumper), and Two Point Incremental Forming (TPIF) (fender, hood, and trunk lid) and rolling (doors) processes. Other studies have focused on structured sheet metals. These are sheets that have already been engineered with specific patterns and ribs to enhance rigidity. Sterzing [17] demonstrated that these structured sheet metals have improved stiffness properties when compared to flat sheets, and Malikov et al. [18] showed that there is a decrease in stiffness whenever the stiffness geometries are removed. It is also important to note that stiffness is not only dependent on the shape (in our case, the stiffness geometries) and size (in our case, the cross-sectional area of the flat sheet metal) but also on the Young's modulus of the material, in which aluminum has good stiffness properties [19].

1.3. Gap Identified

The previous section shows that the application of stiffness geometries on monolithic designs for the deep drawing of large, non-rotational components has not been fully explored. It is also evident that overcoming bulging on large sheet metal products is a huge challenge whenever reinforcements are not used. To the best of the authors' knowledge, the existing monolithic rooftop tents currently available on the market are primarily made from composite materials or plastics, such as Acrylonitrile Butadiene Styrene (ABS) and fiberglass. These types of rooftop tents have a shorter lifespan because they lack structural strength. Also, the plastic material is susceptible to degradation when exposed to direct sunlight for a prolonged time. The effects include: the color fades, the surface cracks and becomes brittle, and the material warps [20]. This makes these types of rooftop tents less durable when compared to aluminum rooftop tents. Hence, the aluminum rooftop tent is a better option for customers who desire a product that is more durable and less cost-effective in the long term. However, the aluminum rooftop tents that are currently available on the market are made of different sheet metal parts that are joined together.

It is against this background that this research presents the development of a monolithic, lightweight, stiffened, non-rotational automotive rooftop tent that is manufactured via the deep-drawing process. It focuses on merging monolithic design, the application of stiffness geometries, and the use of the deep drawing process to produce a one-piece rooftop tent whose performance is not compromised. The research is done under the following specific objectives:

1. To analyze the polyolithic (composed of many parts) rooftop tent design and its limitations.
2. To design a lightweight, monolithic aluminum rooftop tent.
3. To manufacture the lightweight, monolithic aluminum rooftop tent through the deep-drawing process.

The scope of the research is limited to the design of a non-rotational, monolithic sheet metal product that satisfies the following conditions:

- The product must be economically manufactured via the deep-drawing process.
- The product must fulfill its intended purpose under the action of external static or dynamic loads.
- The number of parts, raw material input, and fuel consumption must be reduced.
- Since the product is made for outdoor enthusiasts, it must be manufactured from corrosion-resistant aluminum material.

The rest of the paper is organized as follows: the next section is the materials and methods, where the materials used, product description, and the limitations of the polyolithic rooftop tent are determined through the case study conducted and the development of a monolithic rooftop tent is presented. This is followed by the results and discussion section, where the validation via NX software simulation is presented, followed by validation

through the manufacturing of the rooftop tent via the deep-drawing process. Then follows a discussion of the effects of its production on the limitations that were identified during the case study. After that, the contribution to product design is discussed. Then, the limitations of the study are discussed. The last section gives the conclusions of the paper and an overview of future work.

2. Materials and Methods

2.1. Material

Previous publications from this research work focused on the development of a web-based, scalable material selection decision support system [21]. The system enabled an automated, data-driven selection process for the optimum aluminum material for the rooftop tent and selected the aluminum AA1050. Among the available list of alloys, AA1050 offered the best balance between cost, formability, tensile strength characteristics, hardness characteristics, and corrosion resistance. It is against this background that aluminum AA1050 was used in this research.

AA1050 (99.5% Al) is a commercially pure wrought aluminum. It is lightweight and has high ductility and excellent formability properties. This makes it ideal for applications where weight reduction and ease of forming without failure are important [22]. These are applications where a balance of moderate strength and excellent formability is required [23]. It exhibits good corrosion resistance, and this makes it suitable for outdoor applications [24]. It also has a good appearance (aesthetics), which makes the resulting rooftop tent appealing to customers. The chemical composition and the mechanical properties of the aluminum AA1050 alloy are outlined in Tables 1 and 2 [25].

Table 1. Chemical composition of AA1050 alloy.

Material	Mg	Mn	Cu	Fe	Si	Zn	Ti	Al
% composition	0.05	0.05	0.05	0.4	0.25	0.07	0.05	rest

Table 2. Mechanical properties of AA1050 alloy.

Mechanical Property	Value
Density	2.7 g/cm ³
Modulus of Elasticity	68 GPa
Poisson’s Ratio	0.33
Ultimate Tensile Strength	76 MPa
Yield Strength	28 MPa
Shear Modulus	26 GPa

2.2. Product Description

A rooftop tent is an accessory that is mounted on top of an overlanding vehicle, such as a sports utility vehicle (SUV), to provide shelter during a variety of outdoor excursions, such as camping. This gives the customer a more affordable and efficient “mobile house” that comes with some flexibility that cannot be obtained in a hotel or lodge. A polyolithic rooftop tent is shown in Figure 1.

The popularity of the rooftop tent increased in 2020 during the COVID-19 lockdown period. Hotels and lodges were closed, and social distancing was the order of the day, as the world was looking for solutions to save lives from the pandemic. That was the period when the rooftop tent transitioned from being “one of the many alternatives” to becoming “one of the few or the only alternatives” as far as adventure in the natural environment was concerned. It outperforms traditional tents and recreational vehicles (RVs). In comparison to natural tents, the rooftop tent has better ventilation, which allows free air circulation and keeps it cooler in hot weather conditions. Also, its elevated position offers protection from wild animals, especially at night. When compared with RVs, the rooftop tent offers a

solution that is lighter, and this reduces fuel consumption. The world is going green, and rooftop tents act as a more sustainable solution for outdoor exploration [21]. Since it is mounted on top of a car, it encourages the use of existing infrastructure, that is, the roof of the car, and this reduces material usage and costs.

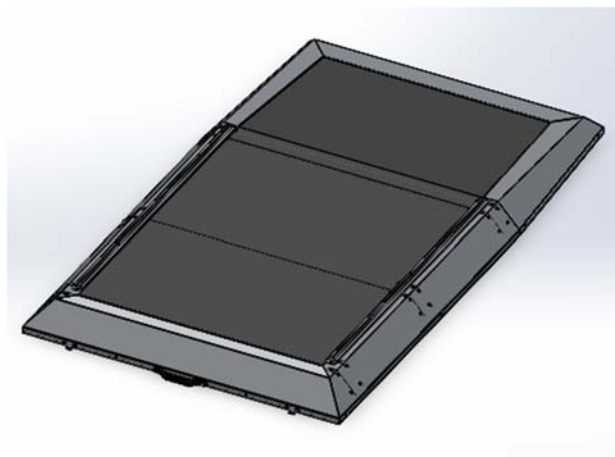


Figure 1. Polyolithic rooftop tent CAD diagram.

Today, the rooftop tent is one of the most preferred alternatives [26]. This is evidenced by its continuous growth in the global market. In 2021, the global rooftop tent market was valued at USD 199.53 million. The projections are that this demand will grow at a compound annual growth rate (CAGR) of 7.76% to a global market value of USD 454.01 million by 2032 [27]. Because it is an outdoor product, the rooftop tent is manufactured from materials that can survive off-road conditions, including humidity, rain, heat, and dust. As such, it is made from metal, composites, or plastics. Metallic rooftop tents are the best where durability is concerned. However, our research has shown that there are no monolithic rooftop tents that are made from aluminum material.

2.3. Case Study: Limitations of Polyolithic Rooftop Tent

A case study was done at ABC Automotive Company. This section briefly outlines the shortcomings and inefficiencies that were identified in this case study. These are, (1) a heavy product, which is made of (2) many individual parts, requiring (3) many process operations, with a possibility of reworking to seal the (4) leaking joints, and resulting in (5) high production time and cost.

1. Heavy product

The polyolithic design is 52.3 kg. This is heavy and necessitates the design of a monolithic design that reduces weight without compromising performance.

2. Many individual parts (polyolithic)

The polyolithic rooftop tent has twenty-three (23) sheet metal parts joined together using the TIG welding, bolting, and riveting processes. Figure 2 shows its exploded view, showing the many parts that are joined together. It also shows the stiffeners, rivets, and bolts. The high number of fasteners increases material handling, requires specialized equipment for operations, and requires huge storage facilities. The TIG welding process needs a lot of energy, manpower, and post-processing. All of this increases the manufacturing costs. This can be eliminated by reducing the number of parts.

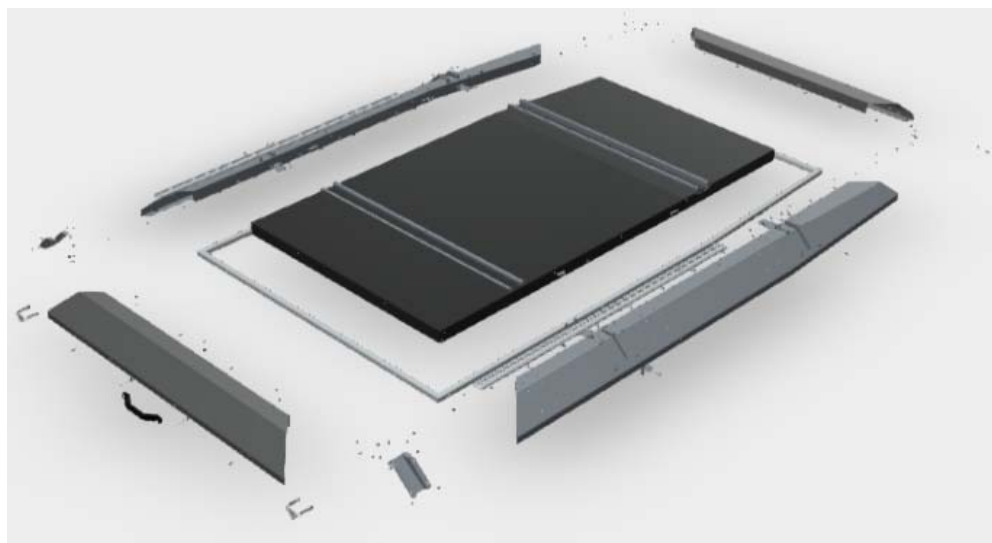


Figure 2. Rooftop tent exploded view.

3. Many operations

The three (3) main manufacturing processes cover the eight (8) different operations that the polyolithic rooftop tent goes through from start to completion.

- (i) Pre-manufacturing: assembly, welding, and finishing.
- (ii) Powder coating: washing and drying, spraying, and curing.
- (iii) Final assembly: final assembly and final quality check.

This increases material handling and inventory costs. Huge storage facilities have been provided for the individual parts, and this further increases the operational costs.

4. High production time

This is a result of many individual parts and many operations that are done to produce the finished product. The time studies and the developed process flow charts for the three (3) main production processes indicate high production time. In addition to that, more time is lost in the laborious manual post-processing of the welded assembly (grinding/polishing to give a smooth surface finish) and the finishing work (cleaning to remove excess Sika Power adhesive). Time studies were conducted, and the total production time to manufacture the polyolithic rooftop tent using the current method is shown in Table 3. Additionally, these processes require an average of fourteen (14) operators.

Table 3. Rooftop tent total production time.

Process	Time (Minutes)
Pre-manufacturing	127.5
Powder coating	118
Final assembly	212
Total production time	457.5

5. Leaking joints

The adhesion process is done during pre-manufacturing using Sika Power 4508 and at final assembly using Sika Flex. The sheet metal, extrusions, and checkered plate sections are first joined using Sika Power and then welded at specific points to improve the structural integrity of the product. It becomes hard when cured with a powder coating. This results in the Sika serving two (2) purposes: firstly, as a sealant, and secondly, to improve the structural integrity of the joint. However, Sika contaminates the weld, and hence, as per company standard operating procedures, it is applied up to 50 millimeters away from

the area that needs to be welded. This eliminates the risk of contamination but creates a problem because the gap between the Sika and the weld is a potential source of leakage. This is a huge issue at the points where the sheet metal meets the extrusion and the checkered plate, that is, where three (3) different parts are joined at one point. Figure 3 shows the gap between Sika Power and the welded joint.

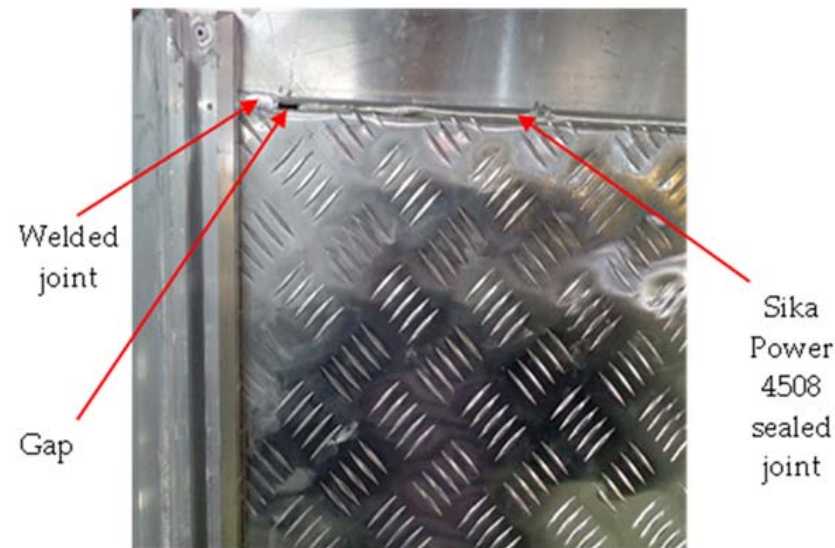


Figure 3. Gap between Sika Power and welded joint.

To minimize the risk of leakage, Sika Flex is applied at the final assembly. However, this does not fully solve the problem because the weld and the cured Sika Power, which is now hard, cause the sheets to stick together, and as such, Sika Flex does not fully penetrate the joint. The quality department has returned a lot of products to the assembly line for additional sealing because they would have failed to pass the water test. Different types of adhesives and sealants have been used to prevent the polyolithic rooftop tent from leaking, but the problem has persisted. The onsite case study showed that the problem does not lie with sealants but with the complexities associated with how to merge the welded section with the adhesive sealant without contaminating the weld or affecting the properties of the sealant, especially on areas where 2 sheets meet an extruded stiffener.

2.4. Design Optimization Methodology

The main objective of the design optimization methodology is to achieve a lightweight, monolithic rooftop tent without compromising structural stiffness. Alternative stiffness geometries were considered, modeled, analyzed, and evaluated. This was done through an iterative simulation-driven approach where various stiffness geometry patterns were evaluated to ensure an optimal balance between the complexity of the stiffness geometries, ease of tool design for the stiffness geometries, symmetry, rigidity, and the overall manufacturing cost. The flow chart in Figure 4 details the process that was used to select the final design, ultimately achieving a monolithic rooftop tent that is manufactured via the deep-drawing process.

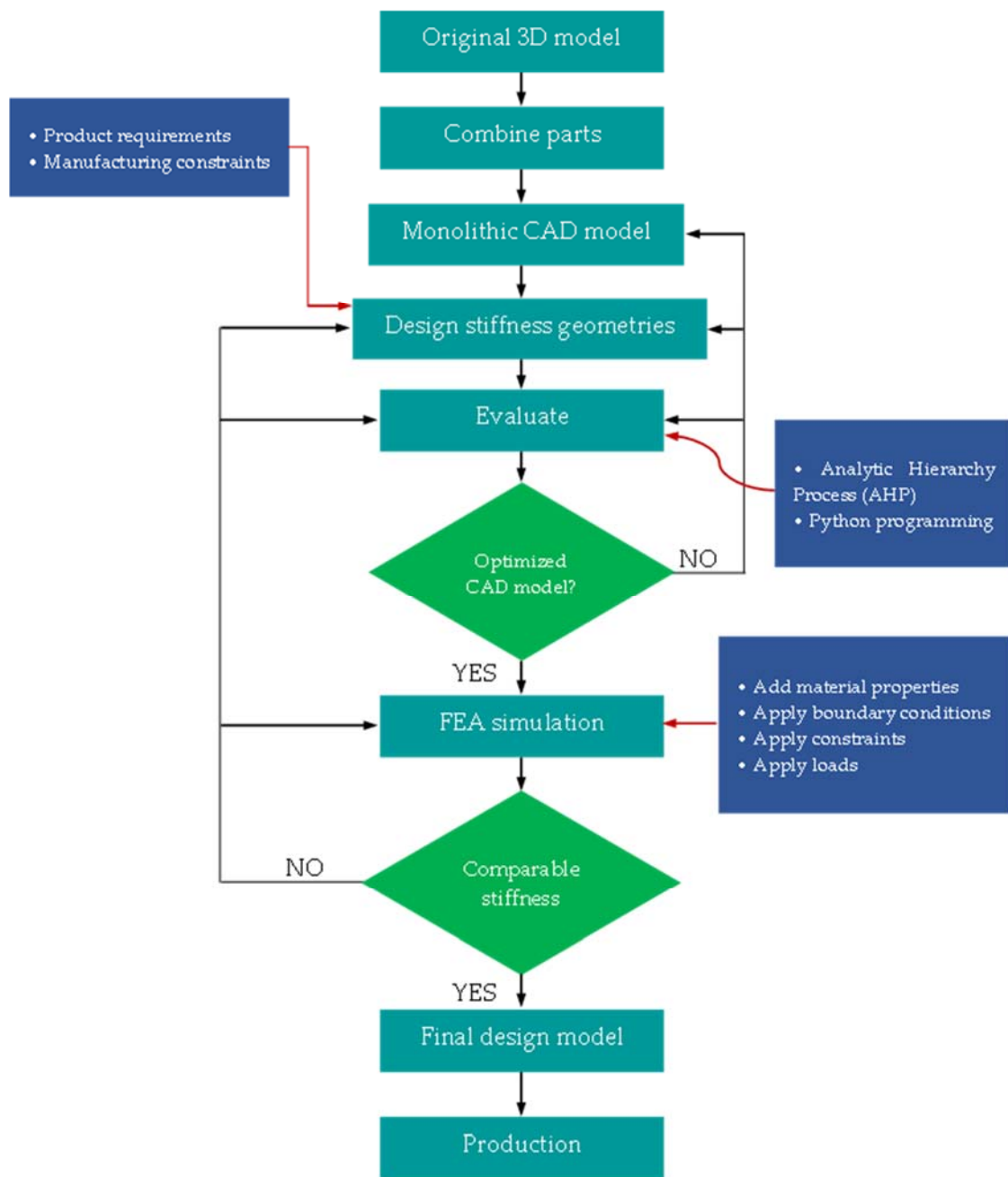


Figure 4. The design optimization methodology for the monolithic rooftop tent.

2.5. Development of the Monolithic Rooftop Tent

The limitations identified in the case study led to the development of the monolithic rooftop tent. The rooftop tent shape was maintained. Any change to the outer dimensions was avoided because the rooftop tent is designed for already manufactured vehicles. It is designed to cater to the Mercedes Benz X Class, Ford Ranger, Land Rover, Toyota Fortuner, Toyota Hilux, Nissan NP300, and Isuzu. Hence, it must be a perfect fit, and any change will result in the need to also change the vehicle’s shape and dimensions. Hence, the polyolithic rooftop tent dimensions are used as the real-life benchmark component. Figure 5 shows the monolithic design.

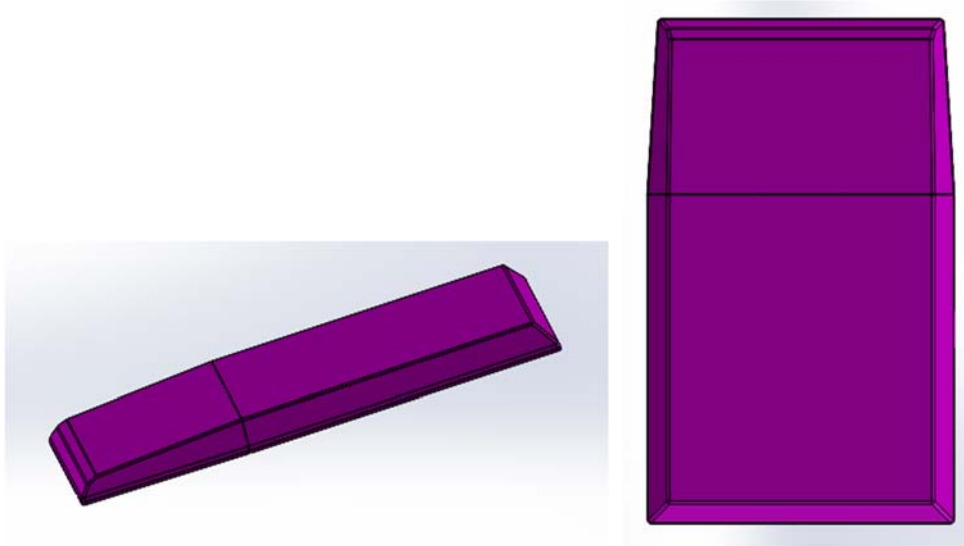


Figure 5. Monolithic design.

2.6. Possible Stiffness Geometry Layouts

To enhance the stiffness of the monolithic rooftop tent, three (3) possible layouts or concepts for the stiffness geometries were developed through NX and SolidWorks 2023 software. This was done while maintaining the same initial shape and dimensions. The material constituent of the aluminum sheet was maintained as AA1050, while the stiffness profiles were varied within a static structural analysis study. This approach reduced the need for thicker materials, thereby maintaining the lightweight nature of the tent. The design process focused on optimizing the shape and distribution of these geometries to ensure that the aluminum sheet metal would exhibit maximum stiffness in critical areas. This method allowed for a more efficient use of material, ensuring that stiffness is achieved without adding unnecessary weight.

2.6.1. Concept 1: Honeycomb

The honeycomb stiffness geometries are shown in Figure 6. This concept leverages the inherent strength and efficiency of honeycomb structures to enhance product stiffness without adding extra material. Honeycomb geometries are known for their exceptional strength-to-weight ratio, making them ideal for reinforcing large, flat sheet metal surfaces that are susceptible to buckling and deformation over time [28]. In this design, the honeycomb stiffness geometries are strategically integrated into critical areas, specifically the top part of a rooftop tent, which is currently reinforced with a checkered plate, center stiffener, and side stiffener. By utilizing honeycomb geometry, the design provides superior rigidity and prevents long-term shape distortion, all while maintaining a lightweight and efficient construction. The careful placement of these stiffness geometries is crucial, as it maximizes the stiffness where it is needed most, ensuring that the product remains durable and resistant to the stresses of regular use. This approach not only enhances the overall strength and longevity of the product but also optimizes material usage, making it a highly effective solution for improving structural integrity in applications where both strength and weight are critical considerations.

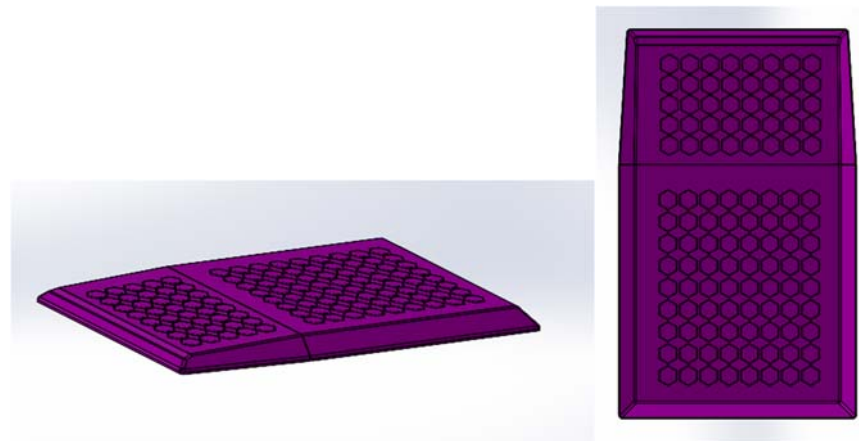


Figure 6. Concept 1: Honeycomb stiffness geometries.

2.6.2. Concept 2: Complex

The complex stiffness geometries are shown in Figure 7. Unlike the honeycomb and parallel stiffness geometries, which rely on simple and uniform shapes, complex stiffness geometries use a variety of shapes, patterns, and placement to increase the stiffness of the rooftop tent. This approach allows for the optimization of the rooftop tent's structural integrity by varying the design of these geometric features. By doing so, the rooftop tent can be precisely tailored to withstand specific loads and stresses, resulting in a more rigid structure. Additionally, the use of complex geometries contributes to reduced material usage, making the tent both stronger and lighter, thereby improving overall performance and efficiency. The main challenge of this concept is the complexity it brings to the tool design for the deep drawing process. The intricate geometries demand more sophisticated tooling. The precision required in the tool design and alignment to accurately and consistently form these intricate geometries is significantly higher compared to simpler geometric patterns, leading to higher costs and longer development times.

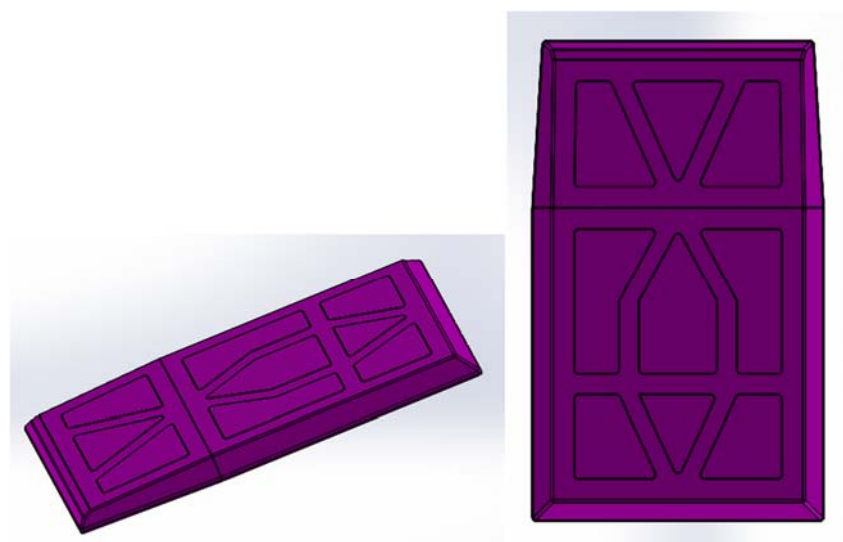


Figure 7. Concept 2: Complex stiffness geometries.

2.6.3. Concept 3: Parallel

The parallel stiffness geometries are shown in Figure 8. In this concept, the integration of flat, corrugated geometries into the rooftop tent's design significantly enhances its structural rigidity and load-bearing capacity. These corrugations are strategically placed on the roof to evenly distribute loads across the tent's surface, making it capable of supporting

additional weight, such as mounted solar panels or storage boxes, without compromising its integrity. The symmetrical positioning of these stiffness geometries ensures a uniform material flow during the manufacturing process, which minimizes the risk of defects like uneven wall thickness, warping, or non-uniform deformation. This symmetry not only simplifies production by reducing the need for complex tooling or multi-stage drawing processes but also lowers production costs and time. In contrast, asymmetrical geometries would create challenges due to uneven material flow, leading to potential defects and increased manufacturing complexity, ultimately making the symmetrical approach more efficient and cost-effective.

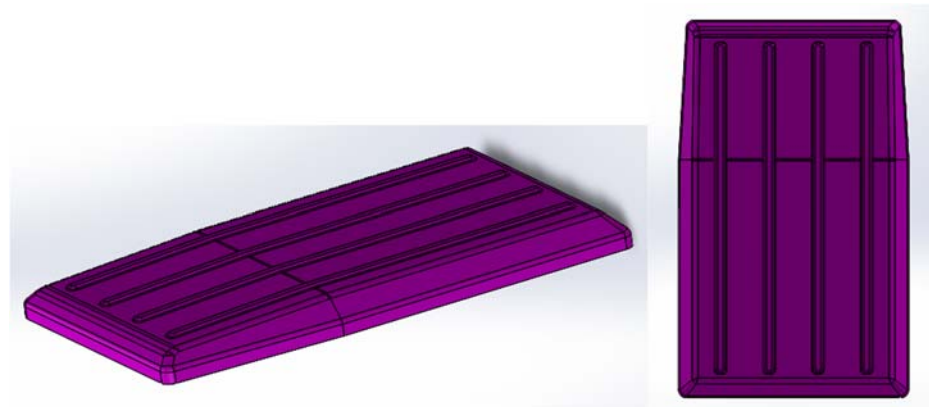


Figure 8. Concept 3: Parallel stiffness geometries.

2.6.4. Analysis of Possible Stiffness Geometry Layouts

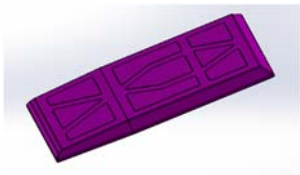
The evaluation of potential stiffness geometry layouts relies on the design guidelines for deep drawing discussed in the previous chapter. The assessment focuses on five key aspects: complexity, tool design, symmetry, rigidity, and manufacturing cost.

- **Complexity:** Intricate geometries can complicate manufacturing and increase the risk of defects, while simpler designs are easier to produce but may sacrifice rigidity or strength.
- **Tool design:** Complex designs need specialized and expensive tooling, whereas simpler designs can use standardized tools, reducing production time and costs.
- **Symmetry:** Symmetrical designs evenly distribute stress and improve material flow during manufacturing, minimizing defects like wrinkles and tears.
- **Rigidity:** It is essential for durability and load bearing. Increased rigidity strengthens the structure but can complicate the design and reduce flexibility.
- **Manufacturing cost:** A balanced design, offering adequate rigidity and symmetry while keeping complexity low, is critical for controlling costs and making the product viable for mass production.

These factors are used in Table 4 to analyze the different concepts of stiffness geometries. The ideal design strikes a balance by offering sufficient rigidity for structural integrity while maintaining symmetry and aesthetic appeal. At the same time, it must avoid excessive complexity, which can drive up costs and make manufacturing more difficult. A design that balances these elements results in a durable, cost-effective, monolithic rooftop tent that is both easy to manufacture and marketable due to its appeal and functionality.

The balance between cost, rigidity, and aesthetics is crucial for market acceptance. If a design is too rigid, it may become complex and expensive to produce. Conversely, too much emphasis on simplicity or aesthetics can compromise the necessary strength required. Therefore, the ability to align these factors effectively determines the rooftop tent's success in the market.

Table 4. Analysis of possible stiffness geometry layouts.

Type	Layout	Evaluation
Honeycomb		<ul style="list-style-type: none"> • Offers exceptional rigidity and efficient load distribution, enhancing structural integrity. However, this increased complexity also drives up production costs because it requires intricate and precise tooling, which is time-consuming and expensive to design and produce. • These geometries are highly effective at distributing stress, leading to excellent strength-to-weight ratios, though there is a higher potential for defects during the manufacturing process. • Ensuring uniform material flow in honeycomb structures is difficult, often resulting in manufacturing defects, such as uneven wall thickness, wrinkles, or material tears.
Complex		<ul style="list-style-type: none"> • Offers increased rigidity, but complicates tool design, making it difficult to scale efficiently, and increasing costs. • Complexity in design can also introduce more points of failure, which affects durability. • Achieving symmetry is difficult, affecting the overall precision and balance of the design. • Uniform material flow is hard to achieve, increasing the risk of uneven wall thickness, wrinkles, or tears.
Parallel		<ul style="list-style-type: none"> • Simpler and more cost-effective design with symmetry that enhances load distribution, though it is less rigid than the honeycomb option. • Improved aerodynamics by allowing smooth airflow between the successive geometries with little resistance. This reduces drag when the tent is mounted on a moving vehicle. • Symmetrical design streamlines the manufacturing process, as it allows uniform drawing and uniform material flow, reduces errors, and enhances reproducibility. • Tool design is simpler and more standardized, leading to lower production costs in comparison to other geometries. • Design is aesthetically pleasing, less error-prone due to its simplicity, and enhances reproducibility.

To systematically determine the most suitable concept, the Analytic Hierarchy Process (AHP) is employed in Section 2.6. This decision-making tool helps prioritize these design factors by comparing them against one another and assigning weights, ensuring a comprehensive evaluation that leads to the most balanced and feasible design choice.

2.7. Evaluation of Possible Stiffness Geometry Layouts

The weights in the matrix were determined using the Analytic Hierarchy Process (AHP), which is a decision-making framework that breaks down complex decisions, prioritizes multiple criteria, and chooses the best alternative based on a structured analysis [29]. It was used in this research to break down the decision into a hierarchy of criteria, such as complexity of the stiffness geometries, ease of tool design for the stiffness geometries, symmetry, rigidity, and the overall manufacturing cost. Pairwise comparisons were made between these criteria to assess their relative importance. The comparisons were then used to construct a comparison matrix, which was normalized to derive the weights. These weights reflected the relative significance of each criterion in the overall decision-making process. The AHP method ensures that the decision is based on a structured and systematic evaluation of all relevant factors.

2.7.1. Steps Involved in Decision-Making

The decision-making process consists of eight (8) steps.

- Step 1: Defining the goal.
- Step 2: Pairwise comparison of the criteria.
- Step 3: Normalizing the matrix.
- Step 4: Calculation of the criteria weights.
- Step 5: Pairwise comparison of the alternatives for each criterion.
- Step 6: Consistency check.
- Step 7: Calculating the global scores.
- Step 8: Ranking the alternatives.

These steps are described in detail in the sections that follow.

2.7.2. Defining the Goal

The goal is to select the optimal stiffness geometry concept for the monolithic rooftop tent that meets the deep-drawing process requirements. This is subject to the following criteria:

- Complexity of stiffness geometries (lower is better).
- Ease of tool design for deep drawing (simpler geometries are better).
- Symmetry of stiffness geometries (higher symmetry is better).
- Rigidity (higher is better).
- Manufacturing cost (lower is better).

2.7.3. Pairwise Comparison of Criteria

The criteria shown in the previous section are balanced to allow the selection of stiffness geometries that not only meet but exceed the necessary standards for both manufacturing efficiency and product performance. The comparison is for the honeycomb, complex, and parallel alternative geometries. The selection hierarchy is illustrated in Figure 9.

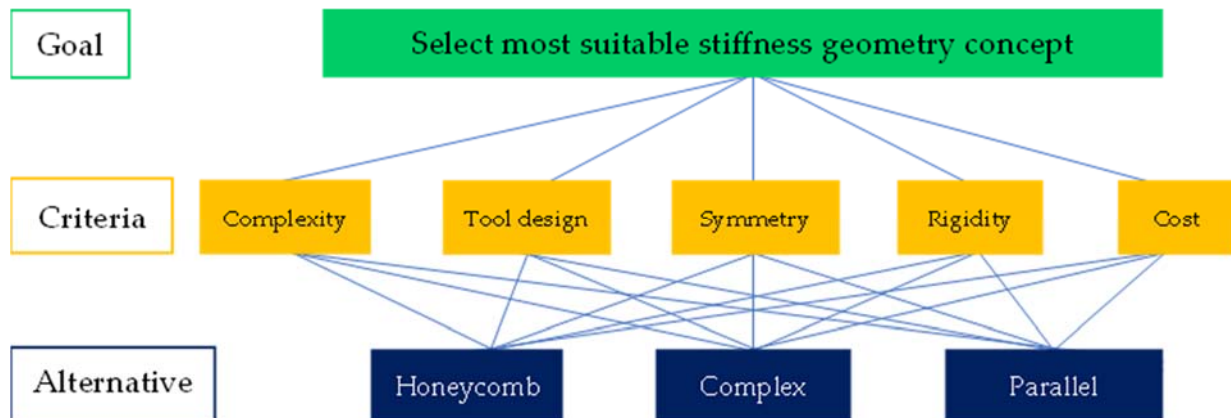


Figure 9. Selection hierarchy.

Complexity, tool design, symmetry, rigidity, and cost are the main considerations in the design and manufacture of the monolithic rooftop tent. Hence, they form the main criteria in the evaluation of the alternatives—honeycomb, complex, and parallel stiffness geometries. Complexity and symmetry influence ease of manufacture, as simpler designs streamline production processes. The tool design directly affects the production cost and time, with more complex tools requiring longer tool-making times and greater financial resources to produce and maintain them. Optimized symmetry and rigidity minimize material waste, ensuring no extra, unnecessary weight is added. Symmetry also enhances load distribution, improving durability and safety while contributing to aesthetic appeal, which is crucial for marketability. Rigidity impacts the load-bearing capacity, determining

the rooftop tent’s durability and reliability. Balancing these factors ensures a durable, cost-effective, and visually appealing product that meets both functional and commercial needs.

A pairwise comparison matrix is constructed, as shown in Table 5. This step focuses on comparing each criterion against the others to determine their relative importance. The pairwise comparison scale typically used in AHP is adopted for this study. The scale is as follows [29]:

- 1: Equally important.
- 3: Moderately more important.
- 5: Strongly more important.
- 7: Very strongly more important.
- 9: Extremely more important.
- 2, 4, 6, 8: Intermediate values.

Table 5. Pairwise comparison matrix.

Criteria	Complexity	Tool Design	Symmetry	Rigidity	Cost
Complexity	1	$\frac{1}{7}$	1	2	$\frac{1}{5}$
Tool design	7	1	4	3	1
Symmetry	1	$\frac{1}{4}$	1	1	$\frac{1}{3}$
Rigidity	$\frac{1}{2}$	$\frac{1}{4}$	1	1	$\frac{1}{2}$
Cost	5	1	3	2	1

This scale is used to create a pairwise comparison matrix. The diagonal elements all have a value of 1 because each concept will be compared to itself. This applies throughout the evaluation process.

2.7.4. Normalizing the Matrix

The values in each column were summed as follows:

- Complexity: $1 + 7 + 1 + \frac{1}{2} + 5 = 14.5$
- Tool design: $\frac{1}{7} + 1 + \frac{1}{4} + \frac{1}{3} + 1 = 2.73$
- Symmetry: $1 + 4 + 1 + 1 + 3 = 10$
- Rigidity: $2 + 3 + 1 + 1 + 2 = 9$
- Cost: $\frac{1}{5} + 1 + \frac{1}{3} + \frac{1}{2} + 1 = 3.03$

Each element was then divided by the corresponding column sum to normalize the matrix. This is shown in Table 6.

Table 6. Normalizing the matrix.

Criteria	Complexity	Tool Design	Symmetry	Rigidity	Cost
Complexity	$\frac{1}{14.5} = 0.069$	$\frac{1/7}{2.73} = 0.052$	$\frac{1}{10} = 0.1$	$\frac{2}{9} = 0.222$	$\frac{1/5}{3.03} = 0.066$
Tool design	$\frac{7}{14.5} = 0.483$	$\frac{1}{2.73} = 0.366$	$\frac{4}{10} = 0.4$	$\frac{3}{9} = 0.333$	$\frac{1}{3.03} = 0.33$
Symmetry	$\frac{1}{14.5} = 0.069$	$\frac{1/4}{2.73} = 0.092$	$\frac{1}{10} = 0.1$	$\frac{1}{9} = 0.111$	$\frac{1/3}{3.03} = 0.11$
Rigidity	$\frac{1/2}{14.5} = 0.034$	$\frac{1/3}{2.73} = 0.122$	$\frac{1}{10} = 0.1$	$\frac{1}{9} = 0.111$	$\frac{1/2}{3.03} = 0.165$
Cost	$\frac{5}{14.5} = 0.345$	$\frac{1}{2.73} = 0.366$	$\frac{3}{10} = 0.3$	$\frac{2}{9} = 0.222$	$\frac{1}{3.03} = 0.33$

2.7.5. Calculation of Criteria Weights

The criteria weights are very important values for calculating the global scores, as detailed in Section 2.7.8. These global scores are then used to determine the overall best alternative. The criteria weights were calculated by averaging the values in each row of the normalized matrix. These weights represent the relative importance of each criterion. They are shown in Table 7.

Table 7. Criteria weights.

Criteria	Weight
Complexity	$\frac{0.069+0.052+0.1+0.222+0.066}{5} = 0.102$
Tool design	$\frac{0.483+0.366+0.4+0.333+0.33}{5} = 0.382$
Symmetry	$\frac{0.069+0.092+0.1+0.111+0.11}{5} = 0.096$
Rigidity	$\frac{0.034+0.122+0.1+0.111+0.165}{5} = 0.106$
Cost	$\frac{0.345+0.366+0.3+0.222+0.33}{5} = 0.313$

Tool design has the highest weight of 0.382. It is the most significant criterion in this analysis, and the stiffness geometries alternatives are compared with the design of the tool as the most critical factor among the criteria considered. Cost has the second highest weight of 0.313. While cost is crucial, it is largely influenced by tool design. Rigidity has a moderate importance of 0.106, suggesting it is a relevant factor but not as critical as tool design or cost. Symmetry has a weight of 0.102, also indicating it has lesser importance in the decision-making process compared to tool design and cost. It, however, affects the rigidity of the product and, hence, the comparable weight. Complexity has a weight of 0.096, which is also comparable to rigidity and symmetry. Overall, tool design leads, followed by cost, then careful consideration of the structural and functional implications of rigidity, symmetry, and complexity.

2.7.6. Pairwise Comparison of Alternatives for Each Criterion

Pairwise comparisons were conducted for the three alternatives—honeycomb, complex, and parallel stiffness geometries—across each criterion: complexity, tool design, symmetry, rigidity, and cost. For each criterion, a pairwise comparison matrix was developed, followed by the normalization of the matrix to calculate the local weights for each alternative. The pairwise comparison matrix for complexity is shown in Table 8.

Table 8. Pairwise comparison matrix for complexity.

Alternative	Honeycomb	Complex	Parallel
Honeycomb	1	5	$\frac{1}{3}$
Complex	$\frac{1}{5}$	1	$\frac{1}{7}$
Parallel	3	7	1

The parallel stiffness geometries are the least complex among the three alternatives, consistently receiving higher preference when compared to both honeycomb (by a ratio of 3:1) and complex (by a ratio of 7:1) stiffness geometries. Honeycomb stiffness geometries are moderately complex and are preferred over complex stiffness geometries (by a ratio of 5:1) but are less preferred than parallel stiffness geometries. Complex stiffness geometries are the most complex, with the lowest preference in comparison to both honeycomb and parallel stiffness geometries. The pairwise matrix is normalized to determine the relative weights (local priorities) of each concept with respect to the complexity criterion, as shown in Table 9.

Table 9. Normalized matrix for complexity.

Alternative	Weight
Honeycomb	$\frac{1/4.2+5/13+0.333/1.476}{3} = 0.283$
Complex	$\frac{0.2/4.2+1/13+0.143/1.476}{3} = 0.073$
Parallel	$\frac{3/4.2+7/13+1/1.476}{3} = 0.643$

The normalized matrix provides the performance score of alternative *i* on criterion *j*. It reflects how well the alternative meets that criterion. This score is then multiplied by

the criterion’s weight, which indicates its relative importance in the overall decision. By summing these weighted scores across all criteria, a global score for each alternative is obtained. The alternatives are then ranked based on their global scores, and a decision is made to determine the most suitable stiffness geometries. The overall interpretation of the complexity criteria is as follows:

- Parallel stiffness geometries (0.643) are the least complex and, therefore, the most favorable option under the complexity criterion.
- Honeycomb stiffness geometries (0.283) are moderately complex, making them less preferable than parallel but more preferable than complex.
- Complex stiffness geometries (0.073) are the most complex and are, therefore, the least preferred option in this analysis.

The normalized weight for the complexity criterion is multiplied by its criteria weight of 0.102 (calculated in Table 7) to compute the global scores. The same applies to all criteria and is detailed in Section 2.7.8. These global scores are then used to determine the overall best alternative. The pairwise comparison matrix for tool design is shown in Table 10.

Table 10. Pairwise comparison matrix for tool design.

Alternative	Honeycomb	Complex	Parallel
Honeycomb	1	3	$\frac{1}{5}$
Complex	$\frac{1}{3}$	1	$\frac{1}{7}$
Parallel	5	7	1

Parallel stiffness geometries are the most preferred in terms of tool design, consistently being preferred over both honeycomb (by a ratio of 5:1) and complex (by a ratio of 7:1) stiffness geometries. This suggests that designing tools for parallel geometries is the simplest or most efficient. Honeycomb stiffness geometries have a moderate preference, being favored over complex (by a ratio of 3:1), but not as much as parallel. This indicates that the tool design for honeycomb is more manageable than for complex stiffness geometries but is still more challenging than for parallel stiffness geometries. Complex stiffness geometries are the least favored alternative, with the lowest preference in comparison to both honeycomb and parallel stiffness geometries. This reflects that tool design for complex stiffness geometries is significantly more challenging or less desirable. The pairwise matrix is normalized to determine the relative weights (local priorities) of each concept with respect to the tool design criterion, as shown in Table 11.

Table 11. Normalized matrix for tool design.

Alternative	Weight
Honeycomb	$\frac{1/6.333+3/11+0.2/1.343}{3} = 0.193$
Complex	$\frac{0.333/6.333+1/11+0.143/1.343}{3} = 0.083$
Parallel	$\frac{5/6.333+7/11+1/1.343}{3} = 0.723$

The overall interpretation of the tool design criteria is as follows:

- Parallel stiffness geometries are the most preferred alternative for tool design, with the highest weight of 0.723.
- Honeycomb stiffness geometries have a moderate weight of 0.193, indicating it is more favorable than complex but not as preferable as parallel.
- Complex stiffness geometries have the lowest weight of 0.083, reflecting that it is the least preferred option regarding tool design.

The pairwise comparison matrix for symmetry is shown in Table 12.

Table 12. Pairwise comparison matrix for symmetry.

Alternative	Honeycomb	Complex	Parallel
Honeycomb	1	$\frac{1}{3}$	$\frac{1}{5}$
Complex	3	1	$\frac{1}{2}$
Parallel	5	2	1

Parallel stiffness geometries are the most preferred in terms of symmetry, as indicated by the highest preference ratios compared to both honeycomb (by a ratio of 5:1) and complex (by a ratio of 2:1). Complex stiffness geometries have a higher preference for symmetry compared to honeycomb (by a ratio of 3:1) but are less preferred compared to parallel. Honeycomb stiffness geometries are the least favored option regarding symmetry. The pairwise matrix is normalized to determine the relative weights (local priorities) of each concept with respect to the symmetry criterion, as shown in Table 13.

Table 13. Normalized matrix for symmetry.

Alternative	Weight
Honeycomb	$\frac{1/9+0.333/3.333+0.2/1.7}{3} = 0.11$
Complex	$\frac{3/9+1/3.333+0.5/1.7}{3} = 0.309$
Parallel	$\frac{5/9+2/3.333+1/1.7}{3} = 0.581$

The overall interpretation of the symmetry criteria is as follows:

- Parallel stiffness geometries are the most preferred alternative with respect to symmetry, with a weight of 0.581.
- Complex stiffness geometries hold a moderate position with a weight of 0.309, indicating it is considered reasonably symmetric but not as much as parallel.
- Honeycomb stiffness geometries are the least preferred alternative concerning symmetry, with the lowest weight of 0.11.

The pairwise comparison matrix for rigidity is shown in Table 14.

Table 14. Pairwise comparison matrix for rigidity.

Alternative	Honeycomb	Complex	Parallel
Honeycomb	1	3	2
Complex	$\frac{1}{3}$	1	$\frac{1}{2}$
Parallel	$\frac{1}{2}$	2	1

The honeycomb stiffness geometries are the most rigid alternative, as they are preferred over both complex (by a ratio of 3) and parallel (by a ratio of 2) stiffness geometries. Parallel stiffness geometries are moderately rigid, preferred over complex (by a ratio of 2), but less rigid than honeycomb. Complex stiffness geometries are the least rigid, with the lowest preference in comparison to both honeycomb and parallel. The pairwise matrix is normalized to determine the relative weights (local priorities) of each concept with respect to the rigidity criterion, as shown in Table 15.

Table 15. Normalized matrix for rigidity.

Alternative	Weight
Honeycomb	$\frac{1/1.833+3/6+2/3.5}{3} = 0.539$
Complex	$\frac{0.333/1.833+1/6+0.5/3.5}{3} = 0.164$
Parallel	$\frac{0.5/1.833+2/6+1/3.5}{3} = 0.3$

Overall interpretation for rigidity criteria:

- Honeycomb stiffness geometries are the most preferred alternative with respect to rigidity, with a weight of 0.539. This suggests that honeycomb is the most structurally rigid, making it the preferred choice when rigidity is a critical factor.
- Parallel stiffness geometries have a moderate weight of 0.3, indicating they are sufficiently rigid but not as much as honeycomb. They are, however, more rigid than complex stiffness geometries.
- Complex stiffness geometries are the least favored alternative regarding rigidity, with the lowest weight of 0.164. This reflects the perception that complex stiffness geometries offer the least rigidity among the three options.

These values are used in further analysis to determine the overall best alternative, considering all criteria. The pairwise comparison matrix for cost is shown in Table 16.

Table 16. Pairwise comparison matrix for cost.

Alternative	Honeycomb	Complex	Parallel
Honeycomb	1	5	$\frac{1}{4}$
Complex	$\frac{1}{5}$	1	$\frac{1}{9}$
Parallel	4	9	1

Parallel stiffness geometries are the most cost-effective alternative and are strongly preferred over both honeycomb (by a ratio of 4) and complex (by a ratio of 9). The high ratios against both alternatives indicate that parallel is considered the least expensive option. The honeycomb stiffness geometries are more expensive than parallel but less expensive than complex (by a ratio of 5), placing it in a middle position concerning cost. Complex stiffness geometries are the most expensive alternative, with the lowest preference ratios compared to both honeycomb and parallel. The pairwise matrix is normalized to determine the relative weights (local priorities) of each concept with respect to the cost criterion, as shown in Table 17.

Table 17. Normalized matrix for cost.

Alternative	Weight
Honeycomb	$\frac{1/5.2+5/15+0.25/1.361}{3} = 0.236$
Complex	$\frac{0.2/5.2+1/15+0.111/1.361}{3} = 0.062$
Parallel	$\frac{4/5.2+9/15+1/1.361}{3} = 0.701$

The overall interpretation of the cost criteria is as follows:

- Parallel stiffness geometries are the most cost-effective option, with a high weight of 0.701. This indicates a strong preference for parallel when cost is the primary consideration, suggesting that it is seen as the least expensive and most affordable option.
- Honeycomb stiffness geometries hold a middle position with a weight of 0.236. It is moderately cost-effective—less so than parallel, but more so than complex.
- Complex stiffness geometries are the least cost-effective alternative, with the lowest weight of 0.062. This suggests that complex stiffness geometries are the most expensive and least desirable from a cost perspective.

The three (3) alternatives of honeycomb, complex, and parallel stiffness geometries have been evaluated based on the criteria of complexity, tool design, symmetry, rigidity, and cost. A consistent check is performed before proceeding to calculate the global scores and determine the most suitable solution.

2.7.7. Consistency Check

The Consistency Ratio (CR) is a measure used in AHP to assess the consistency of the pairwise comparisons made within the decision matrix. It indicates how consistent the judgments have been relative to a random matrix. A CR less than 0.1 means that the comparisons are reasonably consistent, while a CR greater than 0.1 suggests that the judgments may be inconsistent and should be revisited [30]. CR is calculated as shown in Equation (1) [30].

$$CR = \frac{CI}{RI} \tag{1}$$

where

CR: Consistency ratio

CI: Consistency Index

RI: Random Consistency Index

The Consistency Index (CI) is defined as follows [29]:

$$CI = \frac{\lambda_{max} - n}{n - 1} \tag{2}$$

where

CI: Consistency Index.

λ_{max} : The largest eigenvalue of the pairwise comparison matrix.

n : Number of criteria or alternatives.

The largest eigenvalue of a pairwise comparison matrix is calculated using the formula given in Equation (3) [30].

$$\lambda_{max} = \frac{1}{n} \sum_{i=1}^n \frac{(A * Priority\ vector)_i}{Priority\ vector_i} \tag{3}$$

This is for the matrix A, as extracted from Table 5 and shown in Equation (4)

$$A = \begin{pmatrix} 1 & \frac{1}{7} & 1 & 2 & \frac{1}{5} \\ 7 & 1 & 4 & 3 & 1 \\ 1 & \frac{1}{4} & 1 & 1 & \frac{1}{3} \\ \frac{1}{2} & \frac{1}{3} & 1 & 1 & \frac{1}{2} \\ 5 & 1 & 3 & 2 & 1 \end{pmatrix} \tag{4}$$

The transpose A^T of the matrix A is determined using the following set of rules:

- The first row of matrix A becomes the first column of inverse A^T .
- The second row of matrix A becomes the second column of inverse A^T .
- This pattern continues until all rows of matrix A are converted to columns in inverse A^T .

Thus, the transpose, A^T , is given by the matrix shown in Equation (5).

$$A^T = \begin{pmatrix} 1 & 7 & 1 & \frac{1}{2} & 5 \\ \frac{1}{7} & 1 & \frac{1}{4} & \frac{1}{3} & 1 \\ 1 & 4 & 1 & 1 & 3 \\ 2 & 3 & 1 & 1 & 2 \\ \frac{1}{5} & 1 & \frac{1}{3} & \frac{1}{2} & 1 \end{pmatrix} \tag{5}$$

The determinant, $\det(A)$, is calculated using the following formula [30]:

$$\det(A) = (1 * C_{11}) - (7 * C_{12}) + (1 * C_{13}) - \left(\frac{1}{2} * C_{14}\right) + (5 * C_{15}) \tag{6}$$

where C_{ij} : cofactor for the element a_{ij} and is calculated as follows [30]:

$$C_{ij} = (-1)^{i+j} * \det(M_{ij}) \tag{7}$$

where M_{ij} : the 4×4 submatrix obtained by deleting the i th row and j th column from matrix A .

Using Equation (7):

$$\det(A) = -\frac{1}{45} \tag{8}$$

A simplified inverse is as shown in Equation (9).

$$A^T = \frac{1}{56} \begin{pmatrix} 35 & 88 & -432 & 204 & -53 \\ 0 & -672 & 2016 & -1344 & 672 \\ -140 & -128 & 1056 & -480 & 44 \\ 70 & 8 & -192 & 72 & 6 \\ 105 & 600 & -2640 & 1620 & -495 \end{pmatrix} \tag{9}$$

The characteristic polynomial, calculated from Equation (9), is as shown in Equation (10).

$$-\lambda^5 + 5\lambda^4 + \frac{467\lambda^2}{60} - \frac{\lambda}{630} - \frac{1}{45} \tag{10}$$

Simplifying Equation (10), the eigenvalues are:

- $\lambda_1 = 5.27923$
- $\lambda_2 = -0.139717 + 1.20727 i$
- $\lambda_3 = -0.139717 - 1.20727 i$
- $\lambda_4 = 0.05348865$
- $\lambda_5 = -0.0532823$

The sum of the eigenvalues must be equal to the trace [31]. The trace is the sum of the elements on the main diagonal of matrix A . The mathematical model for the trace, modeled using Table 5, can be represented as shown in Equation (11).

$$trace(A) = \sum_{i=1}^5 a_{ii} \tag{11}$$

where the diagonal elements a_{ii} run from $i = 1$ to $i = 5$.

Summing the eigenvalues is as follows:

$$\begin{aligned} \lambda_{total} &= (5.27923) + (-0.139717 + 1.20727i) + \\ &(-0.139717 - 1.20727i) + (0.05348865) + (-0.0532823) \\ &\therefore \lambda_{total} = 5 \end{aligned}$$

Summing the trace is as follows:

$$\begin{aligned} trace(A) &= 1 + 1 + 1 + 1 + 1 \\ &\therefore trace(A) = 5 \end{aligned}$$

Therefore, $\lambda_{total} = trace(A) = 5$.

Python programming was used to verify the answers for the eigenvalues. The NumPy library in Python provides robust functions like `np.linalg.eig()` that accurately compute eigenvalues, ensuring the correctness of results. This is shown in Figure 10.

The programming shows accuracy in the calculation of the eigenvalues.

The largest eigenvalue of the pairwise comparison matrix is $\lambda_{max} = 5.279$.

The Random Consistency Index (RI) is a value obtained from a table based on the size of the matrix (number of criteria).

```
# Define the matrix
A = np.array([
    [1, 1/7, 1, 2, 1/5],
    [7, 1, 4, 3, 1],
    [1, 1/4, 1, 1, 1/3],
    [1/2, 1/3, 1, 1, 1/2],
    [5, 1, 3, 2, 1]
])

# Calculate the eigenvalues
eigenvalues = np.linalg.eigvals(A)
eigenvalues

Result
array([ 5.27923065+0.j          , -0.13971744+1.20727337j,
       -0.13971744-1.20727337j,  0.05348654+0.j          ,
       -0.05328231+0.j          ])
```

Figure 10. Eigenvalue calculation using Python programming.

Therefore,

$$CI = \frac{5.279 - 5}{4} \tag{12}$$

$$\therefore CI = 0.069$$

To determine whether the consistency is acceptable, the consistency index is compared with the Random Consistency Index. From the established values, the RI value for $n = 5$ is 1.11 [32].

$$\therefore CR = \frac{0.069}{1.11}$$

$$\therefore CR = 0.062$$

The Consistency Ratio (CR) is less than 0.1. Therefore, according to the established metrics used to evaluate the reliability of the decision-making matrix [30], the matrix is consistent and reliable for decision-making. The next stage is the calculation of the global scores.

2.7.8. Calculating the Global Scores

The global score, also indicated as the global priority, refers to the overall priority or ranking of an alternative when all criteria have been considered. It combines the local priorities (relative weights of each alternative within each criterion) with the overall importance of the criteria themselves, resulting in a single score for each alternative [29]. This global score is used to determine the most suitable option among the alternatives.

To calculate the global score (or overall score) for each alternative, the performance score of the alternative is multiplied by the weight of the corresponding criterion. This is done for all criteria, and the results are summed to give the global score for each alternative. It is calculated as shown in Equation (13) [29].

$$S_i = \sum_{j=1}^n w_j * a_{ij} \tag{13}$$

where

S_i : Global score for alternative i .

w_j : Weight of the criterion j .

a_{ij} : Performance score of alternative i on criterion j .

The global scores are calculated as shown in Table 18.

Table 18. Global scores.

Alternatives	Complexity (0.102)	Tool Design (0.382)	Symmetry (0.096)	Rigidity (0.106)	Cost (0.313)	Global Score
Honeycomb	$0.283 \times 0.102 = 0.029$	$0.193 \times 0.382 = 0.074$	$0.11 \times 0.096 = 0.011$	$0.633 \times 0.106 = 0.067$	$0.236 \times 0.313 = 0.074$	0.255
Complex	$0.073 \times 0.102 = 0.007$	$0.083 \times 0.382 = 0.032$	$0.309 \times 0.096 = 0.03$	$0.106 \times 0.106 = 0.011$	$0.062 \times 0.313 = 0.019$	0.099
Parallel	$0.643 \times 0.102 = 0.066$	$0.723 \times 0.382 = 0.276$	$0.581 \times 0.096 = 0.056$	$0.26 \times 0.106 = 0.028$	$0.701 \times 0.313 = 0.219$	0.645

2.7.9. Ranking the Alternatives

The global scores indicate the following overall preference:

- Parallel stiffness geometries: 0.645 (most preferred).
- Honeycomb stiffness geometries: 0.255.
- Complex stiffness geometries: 0.099 (least preferred).

Based on the AHP analysis, the parallel stiffness geometries are the most suitable option for the monolithic rooftop tent. This strikes the best balance between minimizing complexity, ease of tool design, achieving symmetry, reducing manufacturing cost, and increasing rigidity for the deep-drawn product. The parallel stiffness geometries have the highest ranking, with a score of 0.645. They scored higher than the honeycomb and the complex stiffness geometries in four (4) criteria: complexity, tool design, symmetry, and cost. This makes the parallel stiffness geometries better placed as the optimal stiffness geometry concept for the monolithic rooftop tent that meets the deep-drawing process requirements. Parallel stiffness geometries strike a balance between cost-effective production and structural integrity. This ensures that the lightweight, monolithic rooftop tent is strong, durable, reliable, and at an affordable price for the customer.

2.8. Monolithic Rooftop Tent Final Design Model

The final design for the monolithic rooftop tent is shown in Figure 11. The stiffness geometries are symmetrically relative to the midpoint of the longest side of the tent. They are also equally spaced, ensuring uniformity in the design, which is important for structural integrity and visual balance. Sharp corners are avoided in accordance with the design for deep-drawing guidelines to improve formability and reduce the risk of material tearing or wrinkling during manufacturing. Thus, the corner radius for the outer shell of the product is 20 mm and 10 mm for the corners of the stiffness geometries. This ensures that the rooftop tent not only meets functional and aesthetic requirements but is also optimized for efficient manufacturing.

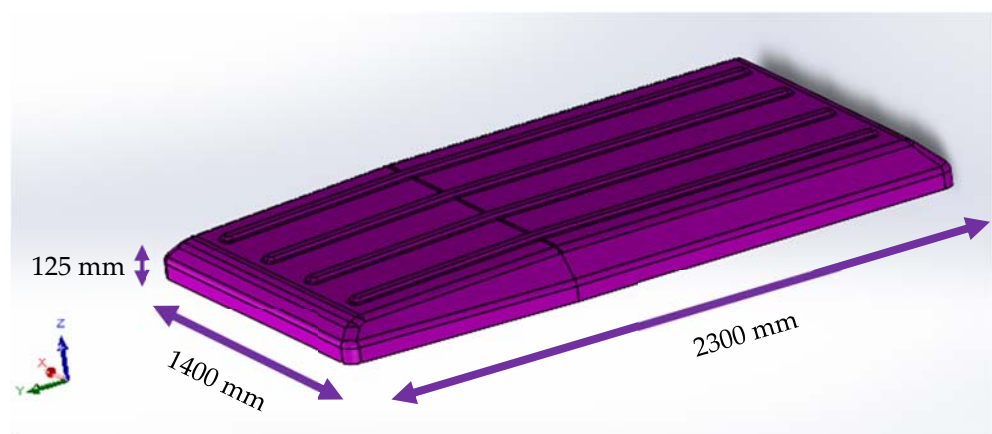


Figure 11. Monolithic rooftop tent final 3D design model.

3. Results and Discussion

3.1. Validation Through Finite Element Analysis (FEA) for Stiffness

A comprehensive Finite Element Analysis (FEA) was conducted using AutoForm sheet metal forming simulation software to verify that the product met performance expectations. The simulation followed these key steps:

- Step 1: Build a 3D model.
- Step 2: Add the material properties.
- Step 3: Apply boundary conditions.
- Step 4: Apply constraints.
- Step 5: Apply loads.
- Step 6: Run the Finite Element Analysis (FEA).
- Step 7: Present results, including stiffness and von Mises.

3.1.1. Build a 3D Model

The geometry of the monolithic rooftop tent was defined through 3D modeling with NX software. The 3D model is shown in Figure 11.

3.1.2. Add the Material Properties

The aluminum AA1050 alloys, the material for the rooftop tent, were used to define the material properties in the simulation. The material properties are listed in Table 2.

3.1.3. Apply Boundary Conditions

A single solid body is selected for meshing, that is, the geometry of the monolithic rooftop tent is the object being analyzed. A 10-node tetrahedral element type (CTETRA10) is used for improved accuracy in capturing the stiffness geometries. Mesh parameters, such as the automatic element size (scaled by 0.5) and surface maximum growth rate (1.3), ensure a finer and more uniform mesh, which is crucial for accurate stress predictions. Mesh quality options, like a Jacobian value of 10, allow for moderate element deformations, while surface mesh settings, such as curvature-based size variation and free-mapped meshing, adapt the mesh to critical high-stress regions. Volume mesh settings, including a smooth gradation factor of 1.05 and a requirement for at least two elements through the thickness, ensure accurate modeling of out-of-plane stresses. Model cleanup options help manage small feature tolerances and avoid excessively small elements that could cause instability. Together, these settings are optimized to balance computational efficiency with accuracy, ensuring that the simulation captures the stiffness and deformation behavior of the rooftop tent during deep drawing. The meshed monolithic rooftop tent section is shown in Figure 12.

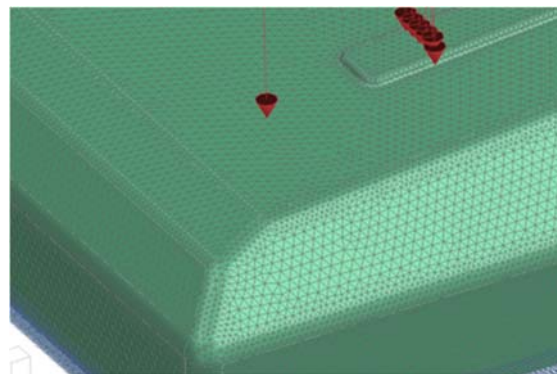


Figure 12. Meshed monolithic rooftop tent section.

A total of 43,046 3D tetrahedral solid units and 89,782 nodes are divided. By breaking down the model into these smaller elements, each element is individually analyzed, and

the result from all elements is aggregated to provide results on the overall behavior of the rooftop tent. This process is essential for accurately predicting how the tent will perform under various stress conditions. The quality of the mesh, including the size and shape of the elements, directly influences the accuracy and efficiency of the simulation, with finer meshes chosen because they yield more precise results regardless of the cost of increased computational resources.

3.1.4. Apply Constraints

The rooftop tent is constrained as shown in Figure 13. The 500 N force is applied in the z-direction (denoted as F_z) across multiple points on the surface of the rooftop tent, as represented by red arrows. These distributed forces simulate the external pressure or load that the monolithic rooftop tent experiences during use. The bottom edge of the structure is constrained, indicated by Fix ($x = y = z = rx = ry = rz = 0$). This means that the structure is fixed in all six degrees of freedom: translation in the x, y, and z directions and rotation about the x, y, and z axes. This rigid constraint prevents any movement or rotation, which simulates a real-world scenario where the rooftop tent is securely attached or supported at the edges.

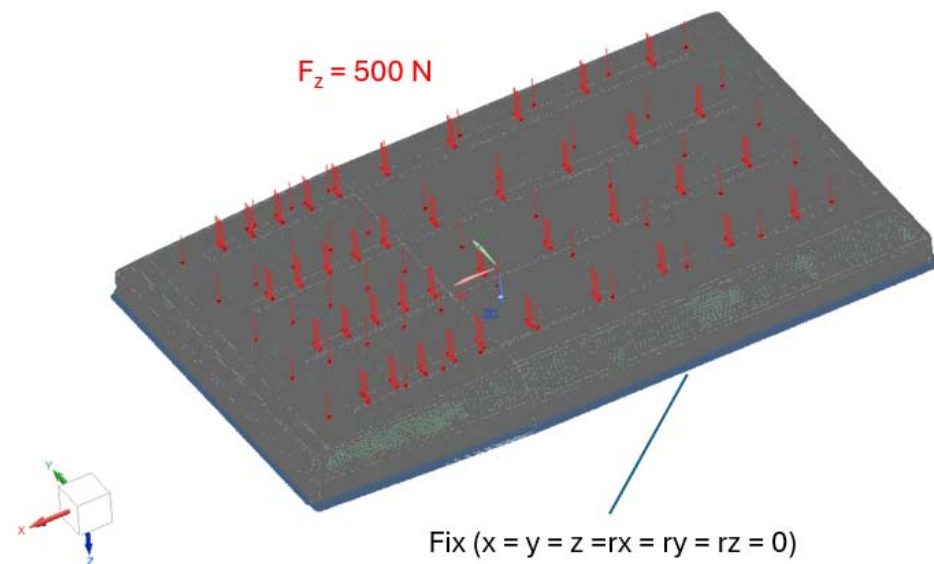


Figure 13. Applying loads.

This setup assesses the structural response and stiffness of the rooftop tent under a uniform load. By applying a force in the z-direction while keeping the edges fully constrained, the simulation can determine how the material and geometry of the rooftop tent distribute the load. The results of this simulation provide insights into how much deformation occurs under the applied load, which is essential for evaluating the tent's stiffness and ensuring it can withstand external pressures, such as mechanical stress, during operation.

3.1.5. Apply Loads

The maximum load under operating conditions is 500 N. This is the same load that the top surface of the monolithic rooftop tent was subjected to in order to assess the displacement under stress. The load is distributed uniformly on the top surface of the rooftop tent. It mirrors the weight capacity of the polyolithic rooftop tent model. Dynamic forces, such as those generated by wind, were not included in the analysis. The reasoning behind this is that if the structure can support the maximum static load of 500 N (according to case study company documents), it should also maintain stability under typical wind conditions, particularly when the vehicle is stationary at a campsite. The ability to withstand

a substantial static load is expected to inherently provide enough structural integrity to resist the dynamic forces encountered in such situations.

3.1.6. Run the Finite Element Analysis (FEA)

The fifth step was to run the simulation. FEA was carried out through the AutoForm sheet metal forming simulation software. AutoForm is a widely used software in the automotive industry (AutoForm Engineering, 2022). It was used to determine the deformation characteristics of the monolithic rooftop tent under the action of forces.

3.1.7. Stiffness Results

The stiffness results for a monolithic rooftop tent provide critical insights into the structure’s ability to withstand external forces and maintain its shape under a load. These results assess the rigidity of the rooftop tent, which directly affects its durability, load-bearing capacity, and overall performance in real-world conditions. High stiffness ensures better load distribution, enhances safety, and minimizes deformation, contributing to the tent’s long-term reliability and functionality. Figure 14 shows the displacement after the application of a 500 N force. A Cartesian coordinate system is depicted, with axes X, Y, and Z labeled, indicating that the displacement is analyzed in the vertical direction (Z-axis).

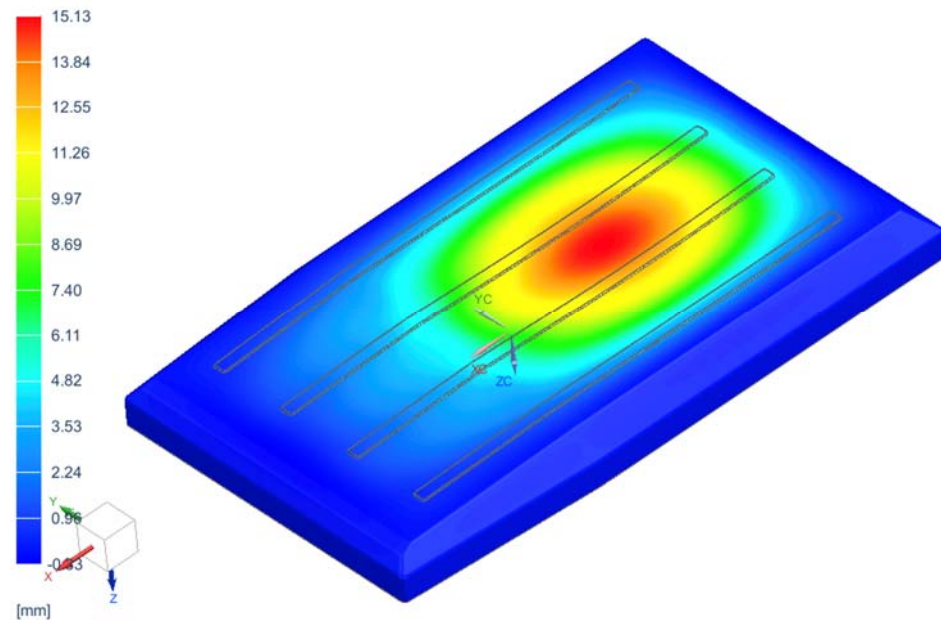


Figure 14. The displacement in the z-direction.

The maximum displacement after the application of a 500 N force is 15.13 mm. The displacement distribution shows that the highest displacement (red zone) occurs in the upper central region, which progressively decreases outward toward the edges. The displacement gradually decreases, transitioning through orange, yellow, green, and finally blue towards the edges, which indicates minimal displacement.

Using the displacement results above, the stiffness for the monolithic rooftop tent can, therefore, be calculated according to Equation (14) [33].

$$k = \frac{F}{\delta} \tag{14}$$

where

k: Stiffness [N/mm]

F: Force [N]

δ: Displacement [mm]

$$\begin{aligned} \therefore k &= \frac{500}{15.13} \\ k &= 33.05 \text{ N/mm} \\ \therefore k &= 33.05 \text{ MN/m} \end{aligned}$$

The next step is to calculate the stiffness per unit weight, which is the ratio of the structure’s stiffness to its mass. This is shown in Table 19.

Table 19. Stiffness per unit weight.

	Calculation	Stiffness per Unit Weight
Weight	33.05 kg	
Stiffness	33.05 MN/m	
	$\frac{33.05 * 10^6}{36.7 * 9.81}$	$9.2 * 10^4$

The simulation results confirm the effectiveness of this design, demonstrating strong resistance to deformation. This provides essential data to ensure the final product meets the required standards for load-bearing capacity and durability.

3.1.8. Von Mises Results

Another important aspect of stiffness analysis is the von Mises stress. This is a measure used to determine if a material will yield (deform permanently) under a complex state of stress. Instead of analyzing the stress in multiple directions, the von Mises criterion converts the multi-axial stress state into a single equivalent stress [34]. This criterion is used to ensure that the monolithic rooftop tent can withstand complex loading without yielding. The results for von Mises stress under the loading of 500 N are shown in Figure 15.

The highest stress, indicated by the yellow and green colors, is concentrated in the middle section of the stiffness geometries. Most of the other areas are largely blue, which indicates lower stress levels. The simulation results show that the location of the stiffness geometry coincides with the section of the rooftop tent that experiences the highest stress concentration, that is, the area likely to experience the greatest deformation. This indicates that the stiffness geometries are functioning as designed, that is, to increase the stiffness in the structure. Also, there is an even spread of stress along these stiffened regions, which shows efficient load-bearing performance. Aluminum AA1050 has a yield strength of 28 MPa [25], which is higher than the maximum stress shown in Figure 15. This means that the monolithic rooftop tent is well within the elastic range. The von Mises stress plot shows that the monolithic rooftop tent structure sustained the 500 N load. The stress concentrated in specific regions of the design shows that the greater part of the product experiences minimal stress. The application of stiffness geometries effectively reinforces the product and reduces the overall deformation. This ensures that the product does not bulge but maintains its integrity when it is subjected to a load.

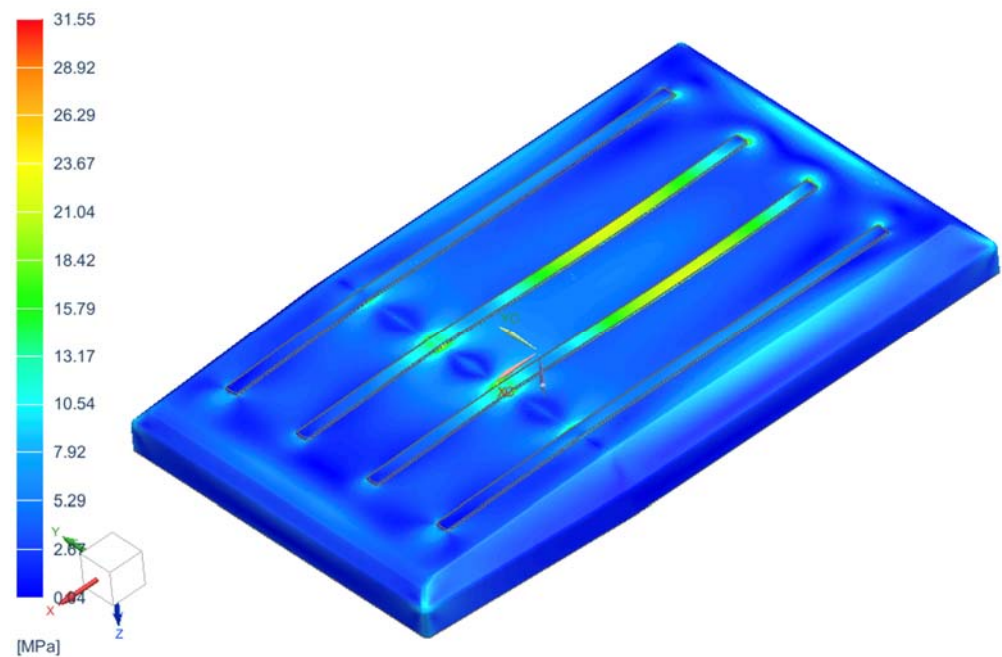


Figure 15. Von Mises stress.

3.2. Validation Through Production via Deep Drawing

The validation process was conducted through the deep-drawing process. The tooling was mounted on the press machine. Before any sheet metal working process can be conducted, the first step is to cut the blank into the required shape and dimensions [35]. Therefore, when the tooling setup was complete, the next step was the aluminum AA1050 blank preparation. The blank was precisely cut using a hydraulic guillotine shear CNC cutting machine. This process was selected because of its ability to perform straight and accurate cuts, it does not alter the microstructure, and it maintains the surface integrity of the material [36]. This enabled a smooth forming process and minimized defects. The cutting process was done following the shape and dimensions as determined by the AutoForm software. This is shown in Figure 16.



Figure 16. The blank cutting in progress (left) and the resulting blank (right).

The prepared blank was taken to the press machine for deep drawing. The position of the tooling and the blank before the punch and die are released are shown in Figure 17.

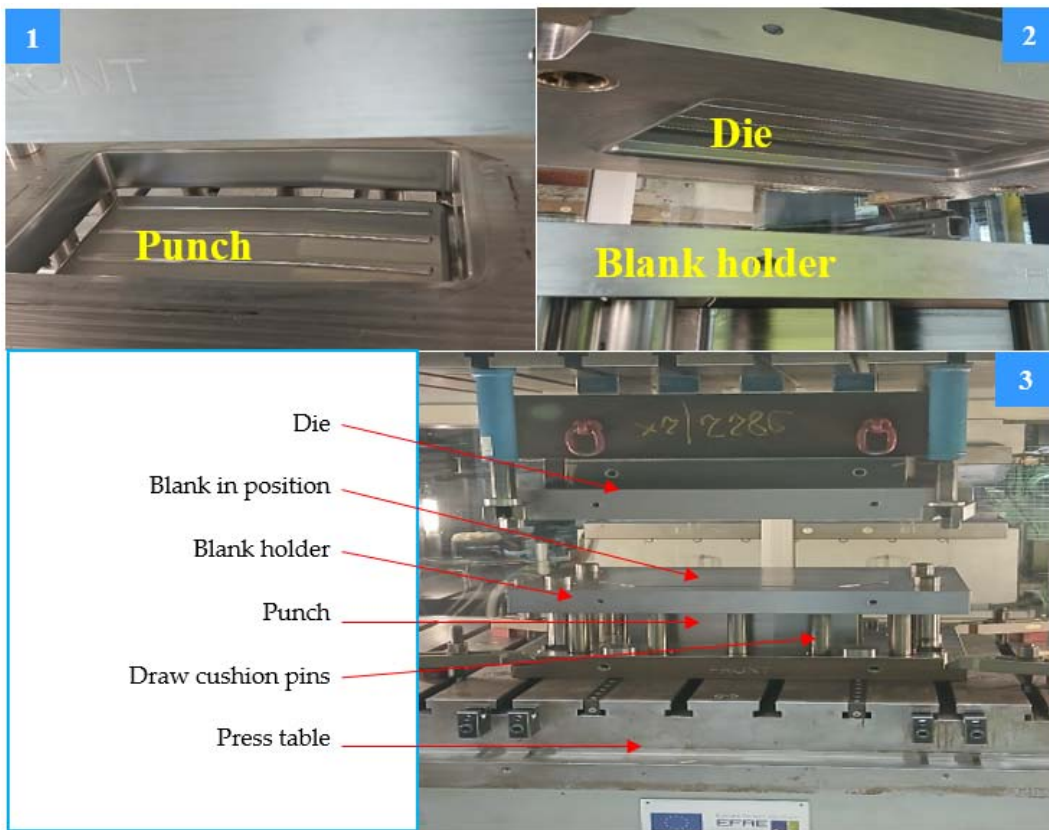


Figure 17. The deep drawing process: (1) the punch, (2) the die and blank holder, and (3) the tooling with a blank in position for deep drawing.

This setup gives the blank sheet proper alignment and stability during the drawing process. This allows precise deformation to ensure consistent wall thickness, which is critical for structural integrity. It also prevents material wrinkling and tearing, especially at the corners. The deep-drawn monolithic rooftop tent, before and after trimming, is shown in Figure 18.



Figure 18. The deep-drawn monolithic rooftop tent, before trimming (left) and after trimming (right).

The deep drawing process was successfully conducted. The material exhibited uniform flow. The rooftop tent had consistent sheet thickness. It had no wrinkles and did not tear. This ensured that structural integrity was obtained.

3.3. Effect of Monolithic Design on the Limitations of Polyolithic Rooftop Tent

The case study explained in the previous section identified five (5) major limitations associated with the production of the polyolithic rooftop tent. These are listed below:

1. Heavy product: the polyolithic design is 52.3 kg.
2. Many individual parts (polyolithic): a total of twenty-three (23) sheet metal parts joined together using TIG welding, riveting, bolting, and adhesive bonding.
3. Many operations: eight (8) different operations are required to produce the rooftop tent.
4. High production time: many operations, leading to an average production time of 127.5 min per product for pre-manufacturing.
5. Leaking joints: resulting in a lot of reworks and returns from customers.

The design and manufacture of a monolithic rooftop tent with stiffness geometries eliminated all the abovementioned limitations. The explanation is as follows.

Firstly, the monolithic design is 36.7 kg. The polyolithic design, on the other hand, is 52.3 kg. The comparison demonstrates a weight reduction of 15.6 kg. The lightweight design contributes to a reduction in fuel consumption and carbon dioxide emissions.

Secondly, the number of sheet metal parts is reduced from twenty-three (23) to one (1). This eliminates twenty-two (22) extra sheet metal parts and influences other factors by reducing weight, reducing potential points of failure, eliminating sources of leakage, reducing the number of operations, and reducing production time.

Thirdly, the main operations of pre-manufacturing assembly, welding, finishing, and the final assembly are replaced by one (1) deep-drawing operation for the monolithic rooftop tent. This eliminates production time, material handling costs, and part scraps. It also eliminates the need for adhesive bonding, TIG welding, riveting, and bolting. Furthermore, it eliminates high energy consumption and post-process heat treatment to relieve residual stresses from the high heat generated by TIG welding.

Fourthly, work study techniques of the method study and time study were conducted during the deep-drawing process of the monolithic rooftop tent. This was done to make comparisons with the results that were obtained from the work study performed on the manufacturing process for the polyolithic rooftop tent. The processes under observation are listed below:

- The blank preparation.
- The deep-drawing process, where the rooftop tent is formed.
- The removal of the formed rooftop tent from the press machine.
- The trimming process to remove the outer edges of the blank that were not formed.

These processes and the related times are represented in the process flow chart that was developed in Figure 19.

The average processing time is 6 min 49 s. On the other hand, the production time for the pre-manufacturing of the polyolithic rooftop tent is 127 min 30 s to 6 min 49 s. The deep-drawing process represents a reduction of production time per product by 120 min 41 s.

Fifthly, Leaking was identified as another major problem, which persisted in spite of huge investments in adhesives. It resulted in most customer returns and negative reviews. The monolithic design eliminated this problem. There are no joints hence, there are no leaking points. A total of one hundred and ninety-two (192) fasteners, whose purpose was to mitigate leaking, were eliminated in the process.

The removal of the AA6016 extrusions leaves AA1050 as the only material used on the rooftop tent. Using a consistent aluminum grade results in uniform material properties for the product. The statistical summary of the comparison of the monolithic versus the polyolithic rooftop tent is shown in Table 21.

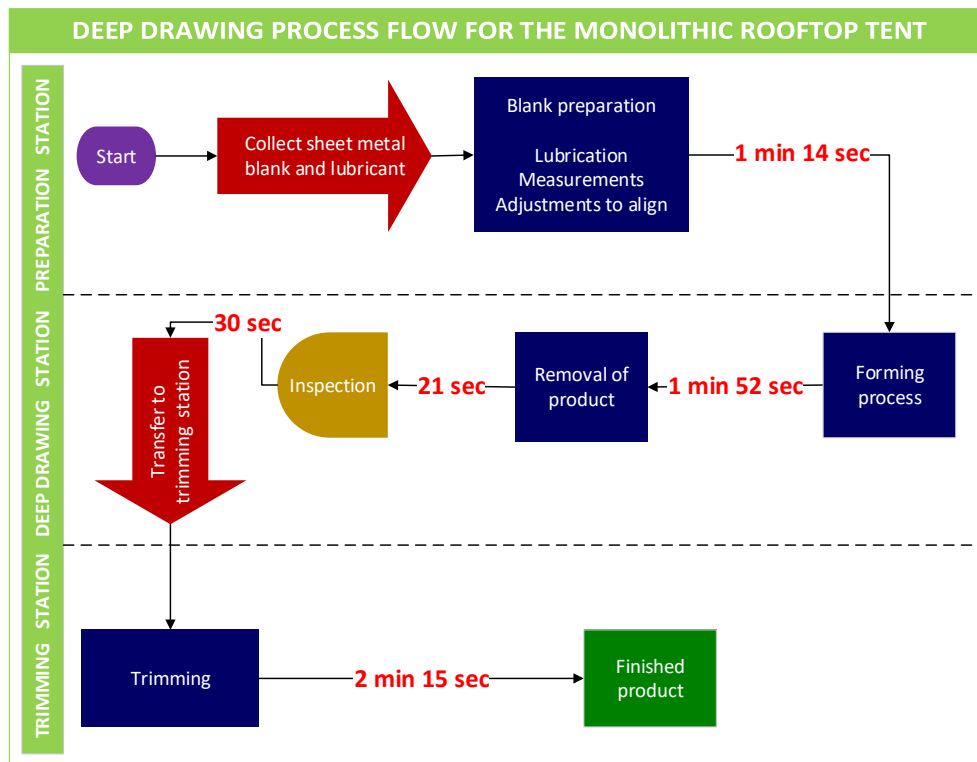


Figure 19. The deep drawing process flow for the rooftop tent.

The summary of the deep-drawing average processing times is tabulated in Table 20.

Table 20. Average deep-drawing times.

Operation	Average Time
Blank preparation	1 min 14 s
Forming process	1 min 52 s
Removal of product	21 s
Inspection	30 s
Trimming	2 min 15 s
Total	6 min 49 s

Table 21. Statistical summary of monolithic versus polylythic rooftop tent.

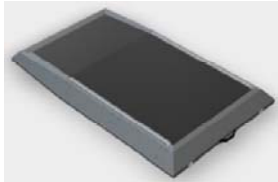
	Polylythic Rooftop Tent	Monolithic Rooftop Tent	Difference
Image			
Weight	52.3 kg	36.7 kg	15.6 kg
Individual sheet metal parts	23	1	22 parts
Number of operations	8	3	5
Production time	127 min 30 s	6 min 49 s	120 min 41 s
Possibility of leaking	Yes	No	No leaking
Material usage	AA1000, AA6000 sheet metal, and AA6061 extrusions	AA1050 sheet metal	No extrusions

Table 21 highlights the advantages of the monolithic rooftop tent in the areas of weight, number of parts, number of operations, production time, the possibility of leaking, material usage, and stiffness per unit mass. These factors show that the monolithic rooftop tent is a better option as far as a lightweight, strong, durable, reliable, and cost-effective product is concerned.

3.4. Economic Analysis

This section discusses an economic analysis of the shift from a polyolithic to a monolithic rooftop tent. This covers the manufacturing costs, maintenance costs, long-term savings, and the overall economic assessment.

3.4.1. Manufacturing Costs

1. Material usage

The monolithic design leads to the reduction of material usage. This leads to substantial cost savings, especially when large production volumes are involved. The cutting and joining together of 23 sheets in the polyolithic rooftop tent results in a lot of offcuts and material waste. This is eliminated by a single deep-drawn monolithic product.

2. Tooling cost

The cost of tooling is another important consideration. The polyolithic rooftop tent requires multiple tools for welding, joining, and assembly. In contrast, the monolithic design uses a single deep-drawing tool. Even though the initial investment in deep-drawing tooling—the press, punch, die, and blank holder—is higher, over time, it is offset by the benefits realized by reducing the production time and labor costs and by eliminating the joining processes of welding, adhesive bonding, bolting, riveting, and their associated tooling requirements [4].

3. Production time

The number of parts is reduced from 23 to 1, and this significantly reduces the production time from 127 min 30 s to 6 min 49 s per product. This results in much higher throughput and efficiency. This reduced cycle time directly impacts operational costs, allowing the company to produce more units in the same time frame.

4. Labor cost

Manufacturing a monolithic rooftop tent via the deep-drawing process reduces the number of processes from eight (8) to three (3). This also eliminates the need for labor-intensive joining methods like welding, bolting, riveting, and adhesive bonding. Consequently, labor costs are reduced due to its simplified assembly and shorter production time.

3.4.2. Maintenance Costs

The monolithic rooftop tent has lower maintenance costs and is more durable. Unlike the polyolithic rooftop tent, it does not have joints, and this eliminates the potential failure points that are associated with joints and fasteners. This is demonstrated by the elimination of leaking, as described in previous sections. Hence, fewer repairs or replacements are needed.

3.4.3. Long-Term Cost Savings

The monolithic rooftop tent reduces weight by 15.6 kg. This translates to a 30% weight reduction without compromising performance. Over time, this weight reduction contributes to improved vehicle fuel efficiency. This benefits the customer (lower fuel costs), the manufacturer (lower manufacturing costs and avoidance of regulatory emission penalties), and the environment (lower carbon emissions) [37].

3.4.4. Overall Economic Assessment

The previous sections have discussed how the transition from the polyolithic rooftop tent to the monolithic rooftop tent reduces material usage, tooling cost, production time, labor cost, and maintenance cost and brings long-term savings. This contributes to an earlier break-even point for the initial investment in the deep-drawing tooling. This results in a financially sustainable, future-proof manufacturing approach that benefits the company and the customer while at the same time meeting the industry demands for efficiency and environmental responsibility.

4. Contribution to Product Design

The research contributes to product design by merging monolithic design, the application of stiffness geometries, and the use of the deep-drawing process to produce a one-piece rooftop tent whose performance is not compromised. The study demonstrates how part count reduction through the monolithic approach is combined with deep-drawing technology to offer a viable pathway to producing lighter, stiffer, more efficient automotive parts without compromising performance. While the combination of the monolithic design and deep-drawing process in the automotive industry is not new, the application to large, non-rotational, stiffened, complex-shaped parts has been underexplored. There is limited existing research specifically targeting the area of monolithic design and stiffening of the non-rotational automotive sheet metal products that are produced via the deep-drawing process. This study, therefore, advances this body of knowledge by combining a comprehensive case study on the design, simulation, and manufacturing of a lightweight, monolithic, stiffened rooftop tent via the deep-drawing process. The research presents an optimized monolithic design that integrates stiffness geometries directly into the product. The significant weight reduction of 30%, reduction of processing routes from eight (8) to three (3), reduction of production time by 120 min 41 s, elimination of leaking, and the integration of stiffness geometries ensure that the monolithic design has the same performance as the polyolithic design and contributes to the originality of the study.

5. Limitations of the Study

This study has several limitations. The simulations that were conducted assume the quasi-static or static forces and exclude dynamic ones, which would relate to wind on a moving vehicle. The rooftop tent is only open for use when the customer requires shelter at a campsite and is closed whenever the vehicle is moving. It is closed for reasons that include the following:

- **Safety:** a closed tent minimizes the risk of it becoming a hazard to other vehicles or pedestrians. An open tent could obstruct visibility or detach from the vehicle, posing dangers on the road.
- **Clearance:** to reduce the overall height of the vehicle, which allows better clearance under bridges, tree branches, and other overhead obstacles.
- **Aerodynamics:** to reduce air resistance and drag. The rooftop tent's closed position is designed to withstand the forces encountered while driving.
- **Protection:** to protect internal components such as bedding, padding on the interior walls, and the canvas tent from any damage that can be caused by weather elements.
- **Security:** to protect personal belongings from falling over and to prevent the entry of any debris.

As a result, the dynamic forces, such as those generated by wind, were not included in the analysis. The results from the simulations show that the structure can support the maximum static load of 50 kg (according to case study company documents). Hence, it should also maintain stability under typical wind conditions, particularly when the vehicle is stationary at a campsite. The ability to withstand a substantial static load is expected to inherently provide enough structural integrity to resist the dynamic forces encountered when the vehicle is in motion.

6. Conclusions and Future Work

This research has presented the design of a lightweight, non-rotational, monolithic automotive rooftop tent. Through a combination of case studies, simulations, and the deep-drawing process, this research demonstrates the significant advantages of transitioning from a polyolithic to a monolithic design for automotive applications. The stiffness geometries were developed to enhance its overall structural integrity without adding unnecessary weight. Alternative layouts were analyzed and evaluated against criteria such as complexity, tool design, symmetry, rigidity, and cost. After a thorough assessment, the most optimal solution was determined to be straight geometries aligned parallel to the tent's longest side. The design contributed to the product design through lightweighting via the reduction in the part count. The following was achieved through the monolithic design:

- The part count was reduced from twenty-three (23) single parts in the polyolithic design to one (1) in the design of an optimized, monolithic, lightweight rooftop tent.
- This monolithic design was 15.6 kg lighter than the polyolithic design. This translates to a 30% weight reduction without compromising performance.
- The processing routes were reduced from eight (8) to three (3).
- The production time was reduced by 120 min 41 s, from 127 min 30 s for the polyolithic rooftop tent to 6 min 49 s for the monolithic rooftop tent.
- Leaking was eliminated.

The results also showed comparable stiffness performance between the lightweight, monolithic rooftop tent and the heavy, polyolithic rooftop tent, providing essential data to ensure the final product meets the required standards for load-bearing capacity and durability. The product was manufactured via the deep-drawing process.

An economic analysis was conducted. It highlights that even though the production of the monolithic rooftop tent may require a huge upfront investment in the deep-drawing tooling—press, punch, die, blank holder—it results in significant long-term cost savings. This is achieved through streamlined production, reduced material and labor costs, and decreased maintenance costs. These benefits position the monolithic design as a cost-effective, sustainable solution in the long run.

Future work includes the following:

- Material testing under typical camping site conditions, such as high temperature, humidity, and dust exposure.
- The non-destructive and destructive testing of the rooftop tent. This involves physical testing under real-use loading conditions, including static and dynamic loads and vibrations.
- The development of a reconfigurable deep-drawing tool for the non-rotational, monolithic rooftop tent. This is critical for further optimizations that will be needed for additional weight reduction, future product improvements, and the addition of other non-rotational products to the production line. A reconfigurable tool can be adjusted to produce different stiffness geometries for different products without requiring an entirely new tool for each configuration. The ability to adapt the tool for other products without new tooling expenses enhances its economic value over time and helps to justify the upfront cost.
- Further application in other products that use different materials and require geometry optimization to reduce weight and production cost.

Author Contributions: Conceptualization, G.P.C.; methodology, G.P.C.; validation, M.N. and G.P.C.; formal analysis, G.P.C. and M.N.; investigation, G.P.C.; resources, S.M., A.S. and M.N.; data curation, G.P.C.; writing—original draft preparation, G.P.C.; writing—review and editing, G.P.C. and S.M.; visualization, G.P.C.; supervision, S.M. and A.S. All authors have read and agreed to the published version of the manuscript.

Funding: This research received no external funding.

Data Availability Statement: Data is contained within the article.

Acknowledgments: The authors would like to extend their gratitude to Stellenbosch University, South Africa, and the Fraunhofer Institute of Machine Tools and Forming Technology IWU, Chemnitz, Germany.

Conflicts of Interest: The authors declare no conflicts of interest.

References

- Chirinda, G.P.; Matope, S. The lighter the better: Weight reduction in the automotive industry and its impact on fuel consumption and climate change. In Proceedings of the 2nd African International Conference on Industrial Engineering and Operations Management, Harare, Zimbabwe, 7–10 December 2020.
- Czerwinski, F. Current Trends in Automotive Lightweighting Strategies and Materials. *Materials* **2021**, *14*, 6631. [[CrossRef](#)] [[PubMed](#)]
- Boothroyd, G.; Dewhurst, P.; Knight, W.A. *Product Design for Manufacture and Assembly*, 3rd ed.; Taylor and Francis Group: New York, NY, USA, 2011; pp. 1–670.
- Chirinda, G.P.; Matope, S.; Sterzing, A. Monolithic design of automobile sheet metal components for the deep drawing process: A review. In Proceedings of the SAIIE32 Proceedings, Gauteng, South Africa, 4–6 October 2021.
- Fusano, L.; Priarone, P.C.; Avalle, M.; De Filippi, A.M. Sheet metal plate design: A structured approach to product optimization in the presence of technological constraints. *Int. J. Adv. Manuf. Technol.* **2011**, *56*, 31–45. [[CrossRef](#)]
- Matope, S.; Chirinda, G.P.; Sarema, B. Continuous Improvement for Cost Savings in the Automotive Industry. *Sustainability* **2022**, *14*, 15319. [[CrossRef](#)]
- Conner, B.P.; Manogharan, G.P.; Martof, A.N.; Rodomsky, L.M.; Rodomsky, C.M.; Jordan, D.C.; Limperos, J.W. Making sense of 3-D printing: Creating a map of additive manufacturing products and services. *Addit. Manuf.* **2014**, *1–4*, 64–67. [[CrossRef](#)]
- Hassan, A.A.; Biswas, B. Topology Optimization of an Automotive Seatbelt Bracket Considering Fatigue. *Designs* **2024**, *8*, 99. [[CrossRef](#)]
- Zhou, J.; Lan, F.; Chen, J.; Lai, F. Uncertainty Optimization Design of a Vehicle Body Structure Considering Random Deviations. *Automot. Innov.* **2018**, *1*, 342–351. [[CrossRef](#)]
- Takagaki, M.; Kato, Y.; Yagi, T. Design of car body by the method of structural optimization. *Q. Rep. RTRI* **2018**, *59*, 37–42. [[CrossRef](#)]
- Hao, J.; Deng, R.; Jia, L.; Li, Z.; Alizadeh, R.; Soltanisehat, L.; Liu, B.; Sun, Z.; Shao, Y. Human-in-the-loop optimization for vehicle body lightweight design. *Adv. Eng. Inform.* **2024**, *62*, 102887. [[CrossRef](#)]
- Chirinda, G.P.; Matope, S.; Sterzing, A. Cars on Weight Loss: The Development of a Methodology for the Topology Optimization of Monolithic Components—Emerging Trends, Challenges and Opportunities. In Proceedings of the 4th European International Conference on Industrial Engineering and Operations Management, Rome, Italy, 2–5 August 2021.
- Yuen, S.C.K.; Nurick, G.N. Experimental and numerical studies on the response of quadrangular stiffened plates. Part I: Subjected to uniform blast load. *Int. J. Impact Eng.* **2005**, *31*, 55–83. [[CrossRef](#)]
- Kleiner, M.; Geiger, M.; Klaus, A. Manufacturing of lightweight components by metal forming. *CIRP Ann.* **2003**, *52*, 521–542. [[CrossRef](#)]
- Bambach, M.; Sviridov, A.; Weisheit, A.; Schleifenbaum, J.H. Case Studies on Local Reinforcement of Sheet Metal Components by Laser Additive Manufacturing. *Metals* **2017**, *7*, 113. [[CrossRef](#)]
- Scheffler, S.; Pierer, A.; Scholz, P.; Melzer, S.; Weise, D.; Rambousek, Z. Incremental sheet metal forming on the example of car exterior skin parts. *Procedia Manuf.* **2019**, *29*, 105–111. [[CrossRef](#)]
- Sterzing, A. Evaluation of Lightweight Construction Potential and Usability of Vaulted Structured Thin Sheets. Ph.D. Thesis, Technische Universität, Chemnitz, Germany, 2005.
- Malikov, V.; Ossenbrink, R.; Viehweger, B.; Michailov, V. Experimental study of the change of stiffness properties during deep drawing of structured sheet metal. *J. Mater. Process. Technol.* **2013**, *213*, 1811–1817. [[CrossRef](#)]
- Stojanovic, B.; Bukvic, M.; Epler, I. Application of aluminum and aluminum alloys in engineering. *Appl. Eng. Lett. J. Eng. Appl. Sci.* **2018**, *3*, 52–62. [[CrossRef](#)]
- Brebu, M. Environmental Degradation of Plastic Composites with Natural Fillers—A Review. *Polymers* **2020**, *12*, 166. [[CrossRef](#)]
- Chirinda, G.P.; Matope, S.; Nagel, M. Development of a material selection decision support system for an automotive application. *Discov. Mech. Eng.* **2024**, *3*, 40. [[CrossRef](#)]
- Davis, J.R. (Ed.) *Alloying: Understanding the Basics*; ASM International: Novetty, OH, USA, 2001.
- Trzepieciński, T.; Najm, S.M. Current Trends in Metallic Materials for Body Panels and Structural Members Used in the Automotive Industry. *Materials* **2024**, *17*, 590. [[CrossRef](#)]
- Ramaswamy, V.; Pareeka, R.; Girib, A.; Anugulab, G.; Srivastavab, V.; Adhikarib, S. Corrosion performance evaluation of aluminum alloys for automotive applications. In Proceedings of the 16th National Congress on Corrosion Control, Kolkata, India, 23–25 August 2012.
- Callister, W.D. *Materials Science and Engineering: An Introduction*, 7th ed.; John Wiley & Sons: Hoboken, NJ, USA, 2007.
- Grand View Research. U.S. Rooftop Tent Market Size & Trends. Available online: <https://www.grandviewresearch.com/industry-analysis/us-rooftop-tent-market-report> (accessed on 15 October 2024).

27. Business Research Insights. Rooftop Tent Market Report Overview. Available online: <https://www.businessresearchinsights.com/market-reports/rooftop-tent-market-102747> (accessed on 15 October 2024).
28. Miller, W.; Smith, C.W.; Evans, K.E. Honeycomb cores with enhanced buckling strength. *Compos. Struct.* **2011**, *93*, 1072–1077. [[CrossRef](#)]
29. Saaty, T.L. Decision making with the analytic hierarchy process. *Int. J. Serv. Sci.* **2008**, *1*, 83–98. [[CrossRef](#)]
30. Malczewski, J. *GIS and Multicriteria Decision Analysis*; John Wiley & Sons: New York, NY, USA, 1999.
31. Schott, J.R. *Matrix Analysis for Statistics*, 3rd ed.; John Wiley & Sons: Hoboken, NJ, USA, 2016.
32. Saaty, T.L. Decision making—The analytic hierarchy and network processes (AHP/ANP). *J. Syst. Sci. Syst. Eng.* **2004**, *13*, 1–35. [[CrossRef](#)]
33. Budynas, R.G.; Nisbett, J.K. *Shigley's Mechanical Engineering Design*, 9th ed.; McGraw-Hill: New York, NY, USA, 2011.
34. Barsanescu, P.D.; Comanici, A.M. *von Mises* hypothesis revised. *Acta Mech.* **2017**, *228*, 433–446. [[CrossRef](#)]
35. Creese, R. *Introduction to Manufacturing Processes and Materials*; CRC Press: New York, NY, USA, 2017.
36. Altan, T.; Tekkaya, A.E. (Eds.) *Sheet Metal Forming: Fundamentals*; ASM International: Novelty, OH, USA, 2012.
37. Chirinda, G.P.; Matope, S.; Zincume, P.; Maisiri, W.; Sterzing, A. Comparative analysis of topology optimization versus material substitution: Is there a best method for vehicle weight reduction? *Procedia CIRP* **2024**, *128*, 132–137. [[CrossRef](#)]

Disclaimer/Publisher's Note: The statements, opinions and data contained in all publications are solely those of the individual author(s) and contributor(s) and not of MDPI and/or the editor(s). MDPI and/or the editor(s) disclaim responsibility for any injury to people or property resulting from any ideas, methods, instructions or products referred to in the content.